University of Kentucky

UKnowledge

Theses and Dissertations--Electrical and Computer Engineering

Electrical and Computer Engineering

2014

FAULT LOCATION ALGORITHMS, OBSERVABILITY AND OPTIMALITY FOR POWER DISTRIBUTION SYSTEMS

Wanjing Xiu
University of Kentucky, blueberryseeds@gmail.com

Right click to open a feedback form in a new tab to let us know how this document benefits you.

Recommended Citation

Xiu, Wanjing, "FAULT LOCATION ALGORITHMS, OBSERVABILITY AND OPTIMALITY FOR POWER DISTRIBUTION SYSTEMS" (2014). *Theses and Dissertations--Electrical and Computer Engineering*. 48.
https://uknowledge.uky.edu/ece_etds/48

STUDENT AGREEMENT:

I represent that my thesis or dissertation and abstract are my original work. Proper attribution has been given to all outside sources. I understand that I am solely responsible for obtaining any needed copyright permissions. I have obtained needed written permission statement(s) from the owner(s) of each third-party copyrighted matter to be included in my work, allowing electronic distribution (if such use is not permitted by the fair use doctrine) which will be submitted to UKnowledge as Additional File.

I hereby grant to The University of Kentucky and its agents the irrevocable, non-exclusive, and royalty-free license to archive and make accessible my work in whole or in part in all forms of media, now or hereafter known. I agree that the document mentioned above may be made available immediately for worldwide access unless an embargo applies.

I retain all other ownership rights to the copyright of my work. I also retain the right to use in future works (such as articles or books) all or part of my work. I understand that I am free to register the copyright to my work.

REVIEW, APPROVAL AND ACCEPTANCE

The document mentioned above has been reviewed and accepted by the student's advisor, on behalf of the advisory committee, and by the Director of Graduate Studies (DGS), on behalf of the program; we verify that this is the final, approved version of the student's thesis including all changes required by the advisory committee. The undersigned agree to abide by the statements above.

<div align="right">

Wanjing Xiu, Student

Dr. Yuan Liao, Major Professor

Dr. Caicheng Lu, Director of Graduate Studies

</div>

FAULT LOCATION ALGORITHMS, OBSERVABILITY AND OPTIMALITY FOR POWER DISTRIBUTION SYSTEMS

_____

DISSERTATION

_____

A dissertation submitted in partial fulfillment of the
requirements for the degree of Doctor of Philosophy in the
College of Engineering at the University of Kentucky

By

Wanjing Xiu

Lexington, Kentucky

Director: Dr. Yuan Liao, Associate Professor of Electrical and Computer Engineering

Lexington, Kentucky

2014

ABSTRACT OF DISSERTATION

FAULT LOCATION ALGORITHMS, OBSERVABILITY AND OPTIMALITY FOR POWER DISTRIBUTION SYSTEMS

Power outages usually lead to customer complaints and revenue losses. Consequently, fast and accurate fault location on electric lines is needed so that repair work can be carried out as fast as possible.

Chapter 2 describes novel fault location algorithms for radial and non-radial ungrounded power distribution systems. For both types of systems, fault location approaches using line to neutral or line to line measurements are presented. It's assumed that network structure and parameters are known, so that during-fault bus impedance matrix of the system can be derived. Functions of bus impedance matrix and available measurements at substation are formulated, from which the unknown fault location can be estimated. Evaluation studies on fault location accuracy and robustness of fault location methods to load variations and measurement errors has been performed.

Most existing fault location methods rely on measurements obtained from meters installed in power systems. To get the most from a limited number of meters available, optimal meter placement methods are needed. Chapter 3 presents a novel optimal meter placement algorithm to keep the system observable in terms of fault location determination. The observability of a fault location in power systems is defined first. Then, fault location observability analysis of the whole system is performed to determine the least number of meters needed and their best locations to achieve fault location observability. Case studies on fault location observability with limited meters are presented. Optimal meter deployment results based on the studied system with equal and varying monitoring cost for meters are displayed.

To enhance fault location accuracy, an optimal fault location estimator for power distribution systems with distributed generation (DG) is described in Chapter 4. Voltages and currents at locations with power generation are adopted to give the best estimation of variables including measurements, fault location and fault resistances. Chi-square test is employed to detect and identify bad measurement. Evaluation studies are carried out to validate the effectiveness of optimal fault location estimator. A set of measurements with one bad measurement is utilized to test if a bad data can be identified successfully by the presented method.

KEY WORDS: distribution systems, fault location observability, optimal fault location estimator, optimal meter placement, ungrounded systems.

_____

Wanjing Xiu
_____

July 19, 2014

FAULT LOCATION ALGORITHMS, OBSERVABILITY AND OPTIMALITY FOR POWER DISTRIBUTION SYSTEMS

By

Wanjing Xiu

Dr. Yuan Liao

_____

Director of Dissertation

Dr. Caicheng Lu

_____

Director of Graduate Studies

July 19, 2014

_____

Date

ACKNOWLEDGEMENTS

I would like to express my sincerest gratitude and appreciation to my dissertation advisor, Dr. Yuan Liao, for his patience and expertise in guiding and helping me overcome every challenge and make steady progress. This dissertation would be impossible without his extensive knowledge and innovative ideas in this field.

I would also like to thank Dr. Paul Dolloff, Dr. Yuming Zhang, Dr. Alan Male and Dr. Zongming Fei, for serving as Doctoral Advisory Committee, and for the invaluable advices they gave.

Thanks to my labmates, Ning Kang, Yan Du, Jiaxiong Chen, Aleksi and Xiangqing Jiao, for their endless support.

Last but not least, I would like to extend my deepest gratitude to my parents and my husband, for their endless love and support.

TABLE OF CONTENTS

LIST OF TABLES

LIST OF FIGURES

Chapter 1 Introductions

At the beginning of this section, a brief introduction to electric power systems is discussed. Afterwards, some of the existing fault location algorithms, mainly on power distribution systems, are reviewed. In the end, the dissertation outline is given.

1.1 Background

An electric power system mainly consists of three essential parts: power generation, power transmission and power consumption. During the transmission of electricity, faults may occasionally occur on electric lines, and cause discontinue of electricity. Fast and accurate fault location methods are needed since they play an important role in accelerating power system restoration, improving system reliability and reducing outage time and revenue losses.

Various reasons may result in power failures. The most common one is the connection between a tree branch and a power line when the tree grows very high and reaches the power line. Severe weather may also bring a fallen tree branch to power lines. Other reasons of faults include animals getting into contact with power lines, climbing inside equipment including transformers and relays. Cable failure due to rain or accidents, and improper actions of circuit breakers and protective equipment may also lead to a fault on power lines.

Faults on power lines are categorized into different types according to how phases of the line and the ground are involved. Generally speaking, there are five types of faults that may occur on power systems, which are listed as follows:

1. Single line to ground faults (LG), including phase A to ground faults (AG), phase B to ground faults (BG) and phase C to ground faults (CG);

2. Line to line faults (LL), including phase A to phase B faults (AB), phase A to phase C faults (AC) and phase B to phase C faults (BC);

3. Double-line to ground faults (LLG), including phase A to phase B to ground faults (ABG), phase A to phase C to ground faults (ACG) and phase B to phase C to ground faults (BCG);

4. Three-phase faults, or line to line to line faults (LLL), including balanced three-phase faults with equal fault impedance and unbalanced three-phase faults with varying fault impedances;

5. Three-phase to ground faults, or line to line to line to ground faults (LLLG), including balanced and unbalanced faults.

1.2 Review of Fault Location Methods for Power Systems

Numerous and diverse fault location algorithms for distribution systems have been developed by researchers in the past to help utilities pinpoint the fault both quickly and accurately.

In most cases, faults occurring on power lines generate transients that propagate along power lines as waves. Those transients travel from the location of the fault to both ends of the faulted line at a speed that is close to the speed of light. The high-frequency component in the waveforms can be detected by protective devices in the time domain. As a result, the time transients take to arrive at each end of the faulty line can be measured. With measured arrival times at both ends and the propagation velocity of the travelling wave, the fault location can be determined. Fault location approaches using travelling wave technologies are proposed in [1] - [5]. Davood et al. make use of the special properties of transients generated by fault to identify the faulted lateral [1]. After

that, fault location is estimated based on wavelet coefficients extracted from voltage phasors. A method to classify fault type and determine fault location in distribution systems with DG is discussed in [3]. Wavelet coefficients of the current measurements are employed in this method. However, many of the existing travelling-wave based fault location algorithms protect only a single line in the power systems. When a certain traveling-wave fault location device is out of order, it may be impossible to locate the fault as usual and the whole system loses its reliability. To overcome this challenge, the time taken for the fault generated transient wave to arrive at every substation with fault location device is recorded [4]. The location of the fault is then calculated by analyzing all recorded data in transmission systems. Similar to [4], [5] is designed for distribution systems with taped loads. Travelling wave arrival time at each bus bars or load terminals are employed to estimate the fault location. Global Positioning System is needed for synchronizing the time at different locations.

Fault location algorithms involving voltage and current measurements have also been studied in the past. When a fault occurs on a power system, voltage magnitudes of power lines may drop for a period of time before the fault clears. This drop is called voltage sag. Fault location approaches based on comparing recorded voltage sag data with a voltage sag database are presented in [6], [7] and [8]. Voltage sag data on all nodes are calculated in advance and prepaid as the voltage sag database. The authors of [9] and [10] pinpoint the location of the fault by making use of voltage sag data and bus impedance matrix. Voltage sags caused by faults are expressed as functions of fault currents and the during-fault bus impedance matrix, which contains the undetermined fault location. By solving the formulated functions, the fault location can be evaluated.

3

Ratan et al. propose a fault location method for radial power systems, where the fault section is identified through an iterative procedure by calculating the modified reactance [11]. The fault point is found when the superimposed fault path current in healthy phase is minimal, which should be zero in the ideal case. André et al. demonstrate an iterative approach for enhanced accuracy of the fault location and no synchronization of measurements at two ends of the line is required [14].

Protection devices have been widely used to aid fault location in power systems. Jinsang et al. extract the magnitude of fault current and fault type from PQ monitoring devices to locate the fault [15]. A method to locate the faulted line section in distribution systems using Fault Indicators (FI) is presented in [16]. After the faulted line is identified, existing fault location methods can be adopted to calculate the fault location. An approach discussed in [17] can be utilized to select the most proper fault location method under a list of limitations and requirements. Jun et al. provide a way to determine fault location based on information available from recording devices and feeder database [18]. Fault locations are ranked and compared with each other to search for the actual fault location.

Approaches to reduce, or eliminate the uncertainty about the fault location in distribution systems are discussed in [19], [20]. A generalized impedance based method was developed in [19]. A potential approach to trim down multiple estimations of fault location was described in [20]. Fault location methods based on intelligent systems, including Artificial Neural Networks (ANN), Fuzzy Logic and Fuzzy Systems, have been proposed in [21] - [26].

Direct circuit analysis is employed to locate faults for distribution systems in [27], [28] and [29]. Special features of distribution systems have been taken into account by researchers in [30] and [31]. Voltage and current phasors at substation are involved to pinpoint faults in [30]. Multiphase laterals and unbalanced conditions are considered in the method. The apparent impedance, defined as the ratio of selected voltage to selected current based on the fault type and faulted phases, has been employed to find the fault location in distribution systems [32]. Damir et al. alter the normal apparent impedance approach to make it suitable for underground distribution lines, which possess special characteristics that do not belong to overhead distribution lines [33]. Useful methods for incipient fault detection and fault location on underground distribution cables are provided in [34], [35] and [36]. A way to determine ungrounded fault location in underground distribution systems by using wavelet transform technique and ANNs for pattern recognition is discussed in [37].

Fault location approaches for ungrounded distribution system have also been studied by scholars as presented in [38], [39] and [40]. Different from grounded distribution systems, there is no intentional neutral wire connection between ungrounded distribution systems and the ground, except the possible measuring devices or high-impedance device [38]. Fault location algorithms for locating single line to ground faults in ungrounded distribution systems are proposed in [38] and [39]. Sequence voltage and current components are employed to identify the fault location in [38]. Pre-fault measurement data and loading condition is not required by [39]. During-fault voltage and current measurements are adopted to determine the faulted feeder, faulted feeder section, faulted line section, fault location successively. Thomas et al. present a fault location

technique by using an injected current signal, which flows to the fault point and return through the ground [40]. The frequency of this signal differs from the frequency of the power line.

Optimal deployment schemes of fault-recording devices have been studied for improved power stability and reliability. Most of the fault location methods developed in the past employ measurements obtained from a limited number of meters installed in a power system. Optimal meter placement in power systems is to make the best use of a limited number of meters available and gives the optimal locations to place these meters. André et al. propose an optimal phasor measurement units (PMU) allocation algorithm for increased fault location accuracy in distribution systems. Monte Carlo simulation is adopted to determine the value of objective function [41]. In each iteration, Greedy Randomized Adaptive Search Procedure yields a greedy randomized solution. Then, the best solution among all solutions is obtained as the result. Other metaheuristic search method, such as Tabu search, is adopted by [42] to achieve the optimal placement of PMUs. Article [43] describes a way to distribute power quality monitors in transmission systems based on nonlinear integer programming technique. FIs are deployed in distributions systems for enhanced service reliability [44]. The combination of costumer interruption cost and the cost of purchasing and installing FIs are minimized to find out the minimal number and installation location of FIs.

Optimal meter placement in power systems, in terms of fault location observability, is to minimize the number of meters needed while keep the entire network observable. According to the definition in [45], if a fault location is called observable, it means this fault location can be uniquely determined with available fault-recording

devices installed in the system. Based on this definition, Lien et al. proposes a method to optimally place PMU in transmission systems for fault location [45]. A travelling-wave based optimal allocation scheme of synchronized voltage sensors is presented in [46]. Kazem et al. present a method to optimally assign PMUs in power systems while achieve fault location observability of the entire network [47]. In this literature, two types of equations: network equations and constraints equations, are formulated based on the physical characteristics of the network and fault type, respectively. Later, the optimization problem is solved by utilizing branch and bound method. Papers that implement the optimal meter placement problem as an integer linear programming problem have been discussed in [48] and [49]. By solving the integer linear programming problem with required constraints, the minimum number of monitors and their best installation locations to pinpoint any fault in the system can be acquired. Voltage measurements are used for optimal meter deployment in transmission systems in [48]. The construction procedure of optimal monitor placement problem has been generalized in [49]. The authors of [50] and [51] introduce methods for allocating FIs for fault location purposes.

Besides algorithms for distribution systems, there has been a great deal of literature about fault location on transmission lines as illustrated in [52], [53], [54] and [55]. However, due to inherent characteristic of distribution systems, like being unbalanced and lack of measuring meters, methods developed for transmission lines are generally not applicable to distribution systems, not to mention ungrounded distribution systems.

1.3 Dissertation Outline

In this dissertation, Chapter 2 will first give a brief introduction of the proposed fault location methods in aspects including the idea of the proposed fault location methods, notations used throughout the dissertation and the procedure to construct bus impedance matrix of the system. Then fault location approaches for both radial and non-radial ungrounded distribution systems are presented. At the end, evaluation studies on both radial and non-radial systems are carried out, and various fault location results are displayed. Chapter 3 describes studies of fault location observability and optimal meter placement in power distribution systems. In the beginning of Chapter 3, the reasons why optimal meter placement methods are needed have been discussed. Afterwards, the procedure to implement fault location observability analysis is illustrated. Optimal meter deployment problem is converted into an integer linear programming problem. By formulating all the required constraints and minimizing the objective function subject to all constrains, the minimal number of meters needed and the optimal locations of those meters can be obtained. In Chapter 3, a way to eliminate fake fault location is also proposed. Evaluation studies have been carried out for fault location observability study and optimal meter placement study on a sample power distribution system. Later, a summary is made at the end of the chapter. Chapter 4 introduces an optimal fault location estimator which makes best of the available measurements. Fault location algorithms are briefly discussed first. Afterwards, optimal fault location estimator and procedure to detect and identify bad measurement are presented. Evaluation studies give the fault location results generated by optimal fault location estimator under various fault conditions. The ability for optimal fault location estimator to find out bad measurement in

all available measurements has been tested. Finally, a conclusion is made in Chapter 5 about the whole fault location study demonstrated in this dissertation.

Chapter 2 Fault Location for Ungrounded Radial and Non-radial Distribution Systems

This chapter extends the idea presented in [10] so that the proposed fault location methods are applicable to ungrounded distribution systems. Chapter 2 is organized as follows. Section 2.1 introduces the methodology of the proposed fault location methods, notations used in the proposed approaches and the procedure to construct bus impedance matrix of the power system. Sections 2.2 and 2.3 presents fault location methods for ungrounded radial distribution systems. Section 2.4 and 2.5 are focusing on fault location algorithms for non-radial ungrounded distribution systems. Measurements at the local substation are utilized to estimate the fault location. In the end, evaluation studies under diverse fault conditions are reported in Section 2.6, followed by the conclusions.

2.1 Introduction

2.1.1 Basic Idea of Proposed Methods

Throughout the dissertation, the terminology "node" is utilized to represent the single-phase connection point in a bus. According to this definition, a bus may have one, two or three nodes according to the number of phases it has [10], [56].

According to the fault type, two, or three fictitious fault nodes are added at the fault points. Then, the bus impedance matrix excluding source impedance but including fault nodes and fault resistances can be derived. Voltages at substation nodes can be formulated with respect to the derived bus impedance matrix and current at the substation. Consequently, voltages at substation nodes can be expressed as functions of fault location, fault resistances and currents at substation. Based on the derived functions, fault location and fault resistances can be obtained. Since the system is ungrounded, fault

location methods for line to line (LL) and three-phase (LLL) faults are derived here. Source impedances are not required by this method [10], [56].
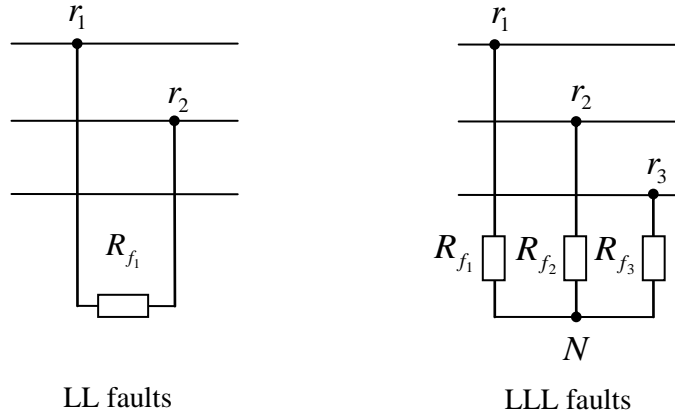
Figure 2.1 Diagrams of LL and LLL faults [10]

The diagrams of LL and LLL faults are shown in Figure 2.1, where fictitious nodes are named r_1, r_2, and r_3, respectively. Corresponding fault resistances are R_{f_1}, R_{f_2}, and R_{f_3}. N is the connection point between three fault resistances in three-phase faults.

2.1.2 Notations Used in the Proposed Fault Location Methods
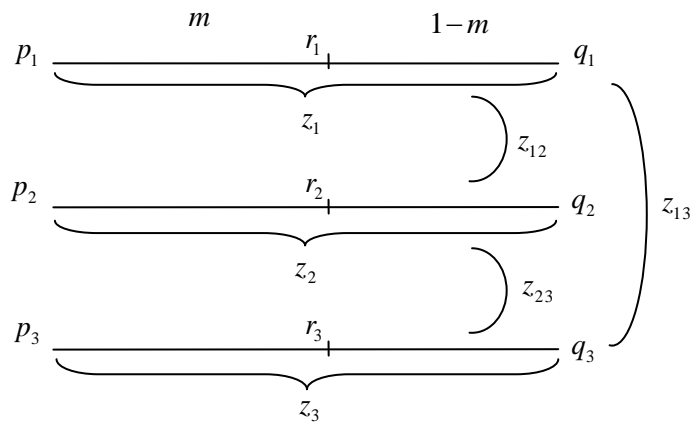
Figure 2.2 Diagram of the faulted section [10]

Suppose that a fault occurs on a three-phase line section as depicted in Figure 2.2. The following notations are used throughout the dissertation.

n total number of nodes of the entire pre-fault network;

$p_1, p_2, p_3, q_1, q_2, q_3$ nodes of two terminals of the faulted line section;

r_1, r_2, r_3 fictitious nodes at fault location, numbered as $r_1 = n+1$, $r_2 = n+2$, and $r_3 = n+3$;

z_1, z_2, z_3 total self-impedance of the feeder between nodes p_1 and q_1, p_2 and q_2, and p_3 and q_3, respectively;

z_{12}, z_{23}, z_{13} total mutual-impedance between different phases of the line section;

m per unit fault distance from bus p;

$[Z_0]$ bus impedance matrix of the original network in phase domain, excluding the fictitious fault nodes, source impedances and fault resistances; it has a size of n by n, whose element in the k_{th} row and l_{th} column is denoted as $Z_{0,kl}$;

$[Z]$ bus impedance matrix of network in phase domain, including the fictitious fault nodes but without source impedances and without fault resistances; It has a size of $(n+3)$ by $(n+3)$, whose element in the k_{th} row and l_{th} column is denoted as Z_{kl};

$E_{p_1}, E_{p_2}, E_{p_3}, E_{q_1}, E_{q_2}, E_{q_3}$ during-fault voltages at node p_1, p_2, p_3, q_1, q_2 and q_3, respectively.

$E_{p_1 0}, E_{p_2 0}, E_{p_3 0}, E_{q_1 0}, E_{q_2 0}, E_{q_3 0}$ pre-fault voltages at node p_1, p_2, p_3, q_1, q_2 and q_3, respectively.

$E_{r_1}, E_{r_2}, E_{r_3}$ during-fault voltages at fault node r_1, r_2 and r_3, respectively.

2.1.3 Construction of Bus Impedance Matrix

Since the network under study is ungrounded, ground cannot be taken as the reference. Thus, the neutral point of the source is taken as the reference node in this chapter. The node voltages are the voltages at the nodes with respect to the reference node.

Pre-fault bus impedance matrix $[Z_0]$ can be constructed using standard bus impedance construction methods as described in [58]. Later, according the fault type, or two, or three fictitious nodes are added to the original network to formulate the during-fault bus impedance matrix $[Z]$. The first n rows and n columns of $[Z]$ are identical to $[Z_0]$. Transfer and driving point impedances are determined as functions of the fault location as follows [10]:

$$Z_{kr_i} = B_{ki} + C_{ki}m, \quad i = 1,2,3 \tag{2.1}$$

$$Z_{r_i r_t} = A_{it\_0} + A_{it\_1}m + A_{it\_2}m^2, \quad i = 1,2,3, \quad t = 1,2,3, \quad and \quad i \neq t \tag{2.2}$$

$$Z_{r_i r_i} = A_{ii\_0} + A_{ii\_1}m + A_{ii\_2}m^2, \quad i = 1,2,3 \tag{2.3}$$

where

Z_{kr_i} : transfer impedance between node k and fault node r_i ;

$Z_{r_i r_t}$: transfer impedance between fault node r_i and r_t ;

$Z_{r_i r_i}$: driving point impedance at fault node r_i ;

Formulas for $B_{ki}, C_{ki}, A_{it\_0}, A_{it\_1}, A_{it\_2}, A_{ii\_0}, A_{ii\_1}$ and A_{ii_2} are shown as follows. They are constants determined by the network parameters [10].

$$B_{ki} = Z_{kp_i} \tag{2.4}$$

$$C_{ki} = -(Z_{kp_i} - Z_{kq_i}) \tag{2.5}$$

$$A_{it\_0} = Z_{p_i p_t} \tag{2.6}$$

$$A_{it\_1} = z_{it} - 2Z_{p_i p_t} + Z_{p_i q_t} + Z_{q_i p_t} \tag{2.7}$$

$$A_{it\_2} = Z_{p_i p_t} + Z_{q_i q_t} - Z_{p_i q_t} - Z_{q_i p_t} - z_{it} \tag{2.8}$$

$$A_{ii\_0} = Z_{p_i p_i} \tag{2.9}$$

$$A_{ii\_1} = z_i - 2Z_{p_i p_i} + 2Z_{p_i q_i} \tag{2.10}$$

$$A_{ii\_2} = Z_{p_i p_i} + Z_{q_i q_i} - 2Z_{p_i q_i} - z_i \tag{2.11}$$

Equations (2.1), (2.2) and (2.3) are applicable to one-phase, two-phase and three-phase line sections.

2.2 Fault Location Methods for Ungrounded Radial Distribution Systems Using Line to Neutral Voltages and Line Currents

Figure 2.3 shows a typical ungrounded radial distribution system, which includes one source, a main feeder, two-phase, three-phase laterals and loads. None of the loads or sources is connected to the ground. In this section, it is assumed that the neutral point of

the source is available, line to neutral voltages and line currents at the substation can be measured. The neutral point of the source is taken as the reference node here. The proposed methods aim to pinpoint the fault location occurring on the network [56].
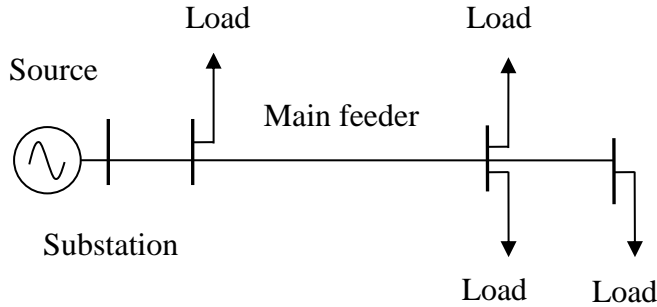
Figure 2.3 A sample ungrounded radial distribution system

Since the original network is ungrounded, the bus impedance matrix of the network excluding the source impedance is non-existent. Hence, a method is proposed here to overcome this challenge, presented as below.
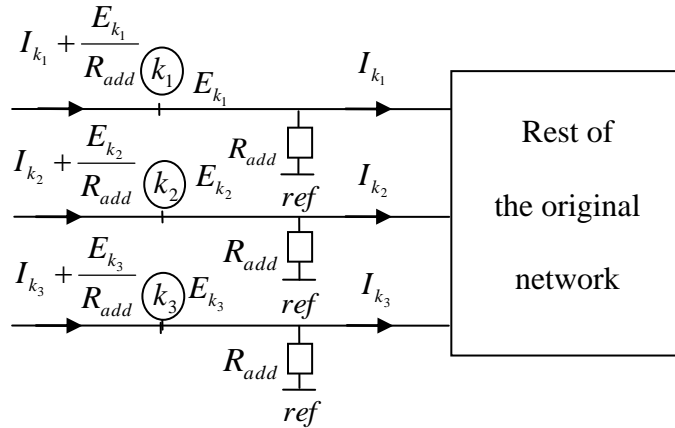
Figure 2.4 Modified ungrounded radial system 1

The original ungrounded system is divided into two parts: voltage source with source impedances and the rest of the network. Figure 2.4 depicts the network without

source impedances, where k_1, k_2 and k_3 denote substation nodes, E_{k_1}, E_{k_2} and E_{k_3} are

during-fault node voltages at substation, and I_{k_1}, I_{k_2} and I_{k_3} are during-fault line currents

at substation.

Three resistances, symbolized as R_{add}, are added between substation nodes and

the reference node ref, as shown in Figure 2.4. R_{add} can be set to any value; a value of

1-ohm is used in this proposed method.

Then, the bus impedance matrix of the modified system as shown in Figure 2.4

can be obtained by following [58]. Bus impedance matrix of the modified network with

fault nodes being added is then acquired as $[Z_M]$. Currents flowing into the modified

network can be calculated from the voltages and currents measured at the substation, as

shown in Figure 2.4. Fault location methods are presented as follows.

2.2.1 LL Faults

Consider an LL fault between phase 1 and 2, which could be any two phases out of phase

A, B and C. Name the nodes corresponding to the faulted nodes at substation as k_1 and

k_2, respectively. Designate $[M]$ as the bus impedance matrix including the fault

resistance of the modified system. $[M]$ can be calculated based on the bus impedance

matrix of modified system without fault resistances $[Z_M]$ [10], [56].

$$[M] = [Z_M] - \frac{[Z_M(:,r_1) - Z_M(:,r_2)][Z_M(:,r_1) - Z_M(:,r_2)]^T}{Z_{M\_r_1r_1} + Z_{M\_r_2r_2} - 2Z_{M\_r_1r_2} + R_{f_1}}, \tag{2.12}$$

16

where $Z_{M\_r_1 r_1}, Z_{M\_r_2 r_2}$ and $Z_{M\_r_1 r_2}$ are driving point and transfer impedances of the modified network, which can be obtained following (2.2) and (2.3). R_{f_1} is the fault resistance between fault nodes r_1 and r_2. T stands for vector/matrix transpose operator.

The voltage at the substation during the fault can be calculated as

$$
\begin{bmatrix} E_{k_1} \\ E_{k_2} \\ E_{k_3} \end{bmatrix} = \begin{bmatrix} M_{k_1 k_1} & M_{k_1 k_2} & M_{k_1 k_3} \\ M_{k_2 k_1} & M_{k_2 k_2} & M_{k_2 k_3} \\ M_{k_3 k_1} & M_{k_3 k_2} & M_{k_3 k_3} \end{bmatrix} \begin{bmatrix} I_{k_1} + \dfrac{E_{k_1}}{R_{add}} \\ I_{k_2} + \dfrac{E_{k_2}}{R_{add}} \\ I_{k_3} + \dfrac{E_{k_3}}{R_{add}} \end{bmatrix}
\tag{2.13}
$$

Equation (2.13) can be expanded into three equations, and each equation contains fault location m and fault resistance R_{f_1}. By rearranging any of the expanded equation, R_{f_1} can be expressed as a function of m. Since R_{f_1} is a real number, R_{f_1} is equal to the complex conjugate of R_{f_1}, from which an equation containing only variable m is obtained. After solving m, and substituting the value of m into the utilized equation, we can also acquire the value of R_{f_1} [10].

2.2.2 LLL Faults

For an LLL fault, define $[S]$ as the bus impedance matrix including the fault resistances. The procedure to obtain $[S]$ based on $[Z_M]$ is demonstrated through (2.14) to (2.16) [10]:

$$
[Z_M^{(1)}] = \begin{bmatrix} [Z_M] & Z_M(:,r_1) \\ Z_M(r_1,:) & Z_{M\_r_1 r_1} + R_{f_1} \end{bmatrix}
\tag{2.14}
$$

$$[Z_M^{(2)}] = [Z_M^{(1)}] - \frac{[Z_M^{(1)}(:,r_2) - Z_M^{(1)}(:,r_N)][Z_M^{(1)}(:,r_2) - Z_M^{(1)}(:,r_N)]^T}{Z_{M\_r_1r_1} + Z_{M\_r_2r_2} - 2Z_{M\_r_1r_2} + R_{f_1} + R_{f_2}}$$ (2.15)

$$[S] = [Z_M^{(2)}] - \frac{[Z_M^{(2)}(:,r_3) - Z_M^{(2)}(:,r_N)][Z_M^{(2)}(:,r_3) - Z_M^{(2)}(:,r_N)]^T}{Z_{M\_r_3r_3}^{(2)} + Z_{M\_r_Nr_N}^{(2)} - 2Z_{M\_r_3r_N}^{(2)} + R_{f_3}}$$ (2.16)

where R_{f_1}, R_{f_2} and R_{f_3} are corresponding fault resistances shown in Figure 2.1. r_N is the node number assigned to the common connection point N of the three fault resistances under three-phase faults, and $r_N = n + 4$.

The voltages at the substation are derived as

$$\begin{bmatrix} E_{k_1} \\ E_{k_2} \\ E_{k_3} \end{bmatrix} = \begin{bmatrix} S_{k_1k_1} & S_{k_1k_2} & S_{k_1k_3} \\ S_{k_2k_1} & S_{k_2k_2} & S_{k_2k_3} \\ S_{k_3k_1} & S_{k_3k_2} & S_{k_3k_3} \end{bmatrix} \begin{bmatrix} I_{k_1} + \dfrac{E_{k_1}}{R_{add}} \\ I_{k_2} + \dfrac{E_{k_2}}{R_{add}} \\ I_{k_3} + \dfrac{E_{k_3}}{R_{add}} \end{bmatrix}$$ (2.17)

Based on equation (2.17), fault location and fault resistances can be acquired as follows. Define $X = [m, R_{f_1}, R_{f_2}, R_{f_3}]^T$ as the unknown variable vector. From (2.17), three functions of the unknown variables are acquired as follows:

$$f_1(X) = E_{k_1} - S_{k_1r_1}(I_{k_1} + E_{k_1}/R_{add}) - S_{k_1r_2}(I_{k_2} + E_{k_2}/R_{add}) - S_{k_1r_3}(I_{k_3} + E_{k_3}/R_{add}) = 0$$ (2.18)

$$f_2(X) = E_{k_2} - S_{k_2r_1}(I_{k_1} + E_{k_1}/R_{add}) - S_{k_2r_2}(I_{k_2} + E_{k_2}/R_{add}) - S_{k_2r_3}(I_{k_3} + E_{k_3}/R_{add}) = 0$$ (2.19)

$$f_3(X) = E_{k_3} - S_{k_3r_1}(I_{k_1} + E_{k_1}/R_{add}) - S_{k_3r_2}(I_{k_2} + E_{k_2}/R_{add}) - S_{k_3r_3}(I_{k_3} + E_{k_3}/R_{add}) = 0$$ (2.20)

Define function vector $F(X)$ as

$$F(X) = [real(f_1), imag(f_1), real(f_2), imag(f_2), real(f_3), imag(f_3)]^T \qquad (2.21)$$

where, *real*(.) and *imag*(.) represent the real and imaginary part of its argument, respectively.

Then, the unknown variables can be obtained iteratively through the following procedure [59]:

$$H = \frac{\partial F(X_n)}{\partial X} \qquad (2.22)$$

$$\Delta X = -H^{-1} F(X_n) \qquad (2.23)$$

$$X_{n+1} = \Delta X + X_n \qquad (2.24)$$

where

X_n is the variable vector for n_{th} iteration;

ΔX is the difference between X_n and X_{n+1};

H is the Jacobian matrix.

Each element in the Jacobian matrix is calculated from the available node voltages and line currents at substation, as long with line impedances.

The iterations can be terminated when the biggest element of the unknown variable update is smaller than the desired tolerance.

2.3 Fault Location Methods for Ungrounded Radial Distribution Systems Using Line to Line Voltages and Line Currents

This section develops an alternative method for fault location, when line to neutral voltages is not available, but line to line voltages are available. Methods for both LL and LLL faults are described.

2.3.1 LL Faults
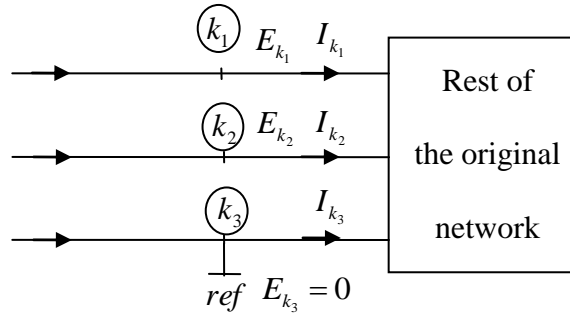
Figure 2.5 Modified ungrounded radial system 2

To construct the bus impedance matrix, one node at the substation, say node k_3, is selected as the reference point, as shown in Figure 2.5. Accordingly, phase to phase voltages can be converted to phase to reference point voltages. The bus impedance matrix of the original network without source impedances, but with the fictitious fault nodes added, $[Z_M]$, can be obtained similarly as in Section 2.2.

Consider an LL fault between phase 1 and 2, which could be any two phases out of phase A, B and C. Name the nodes corresponding to the faulted nodes at substation k_1 and k_2, respectively. The bus impedance matrix of modified system $[M]$, including the fault resistance, can be formulated based on $[Z_M]$ as shown in (2.12).

20

The during-fault line to line voltages at substation nodes are expressed as follows:

$$E_{k_1} = M_{k_1 k_1} I_{k_1} + M_{k_1 k_2} I_{k_2} \qquad (2.25)$$

$$E_{k_2} = M_{k_2 k_1} I_{k_1} + M_{k_2 k_2} I_{k_2} \qquad (2.26)$$

Note that node k_3 is selected as the reference node. E_{k_1} and E_{k_2} are voltages of node k_1 and k_2 with reference to node k_3.

By separating any of the above equations into real and imaginary parts, two real equations can be obtained, from which fault location and fault resistance can be estimated.

2.3.2 LLL Faults

The bus impedance matrix $[S]$, of the network without source impedances, but with the fault resistances, is constructed using equations through (2.14) to (2.16).

The following equations can be acquired based on Figure 2.5.

$$E_{k_1} = S_{k_1 k_1} I_{k_1} + S_{k_1 k_2} I_{k_2} \qquad (2.27)$$

$$E_{k_2} = S_{k_2 k_1} I_{k_1} + S_{k_2 k_2} I_{k_2} \qquad (2.28)$$

Similar to Section 2.2.2, the fault location and fault resistances can be solved by applying the iterative method to equations (2.27) and (2.28) with defined known variable vector X and function vector $f(X)$.

2.4 Fault Location Methods for Ungrounded Non-Radial Distribution Systems Using Line to Neutral Voltages and Line Currents

Different from ungrounded radial distribution system, ungrounded non-radial distribution system have an additional source, called remote source, as drawn in Figure 2.6.
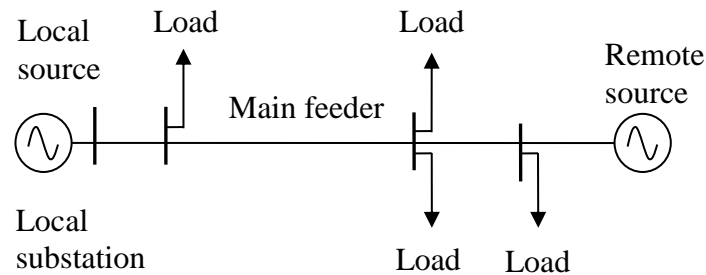
Figure 2.6 A sample ungrounded radial distribution system [56]

In the proposed method, it is assumed that the line to neutral voltages and line currents at the local substation are available. Type I fault location methods proposed in [10] are applied to ungrounded distribution system in this section. Fault location method for LL faults will be illustrated here as an example. Detailed approach for LLL faults can be referred to [10], [56].

2.4.1 LL Faults

Consider an LL fault between phase 1 and 2, which could be phase A and B, or phase B and C, or phase C and A. Designate the nodes corresponding to the faulted phases at local substation as k_1 and k_2. The voltage change due to the fault at node k_1, or superimposed voltage at node k_1, is determined by the transfer impedances and fault currents as follows [10]:

$$\Delta E_{k_1} = E_{k_1} - E_{k_1 0} = -Z_{k_1 r_1} I_{f_1} - Z_{k_1 r_2} I_{f_2} \qquad (2.29)$$

Fault currents under LL faults can be obtained by the following form [10], [60]:

$$I_{f_1} = -I_{f_2} = \frac{E_{r_1 0} - E_{r_2 0}}{Z_{r_1 r_1} + Z_{r_2 r_2} - 2Z_{r_1 r_2} + R_{f_1}} \qquad (2.30)$$

where

R_{f_1} fault resistance between node r_1 and r_2.

From Figure 2.2, pre-fault voltages at fault node r_1 and r_2 are determined as

$$E_{r_1 0} = E_{p_1 0} - m(E_{p_1 0} - E_{q_1 0}) \qquad (2.31)$$

$$E_{r_2 0} = E_{p_2 0} - m(E_{p_2 0} - E_{q_2 0}). \qquad (2.32)$$

Substituting (2.30), (2.31) and (2.32) into (2.29), the following equation is yielded.

$$\Delta E_{k_1} = [(1-m)(E_{p_1 0} - E_{p_2 0}) + m(E_{q_1 0} - E_{q_2 0})]$$
$$\times \frac{[(B_{k_1 2} - B_{k_1 1}) + (C_{k_1 2} - C_{k_1 1})m]}{[(A_{11\_0} + A_{22\_0} - 2A_{12\_0}) + (A_{11\_1} + A_{22\_1} - 2A_{12\_1})m + (A_{11\_2} + A_{22\_2} - 2A_{12\_2})m^2 + R_{f_1}]}$$
$$(2.33)$$

Equation (2.33) is a complex equation, which can be separated into two real equations. There are two unknowns m and R_{f_1}. R_{f_1} is eliminated first and then an equation involving only m is derived, from which m can be obtained. Then R_{f_1} can also be calculated.

2.4.2 LLL Faults

Define $X = [m, R_{f_1}, R_{f_2}, R_{f_3}]^T$ as the unknown variable vector. According to the method described in [10], three functions of the unknown variable vector can be obtained as follows:

$$f_1(X) = \Delta E_{k_1} + Z_{k_1 r_1} I_{f_1} + Z_{k_1 r_2} I_{f_2} + Z_{k_1 r_3} I_{f_3} = 0 \tag{2.34}$$

$$f_2(X) = \Delta E_{k_2} + Z_{k_2 r_1} I_{f_1} + Z_{k_2 r_2} I_{f_2} + Z_{k_2 r_3} I_{f_3} = 0 \tag{2.35}$$

$$f_3(X) = \Delta E_{k_3} + Z_{k_3 r_1} I_{f_1} + Z_{k_3 r_2} I_{f_2} + Z_{k_3 r_3} I_{f_3} = 0. \tag{2.36}$$

By solving equations (2.34), (2.35) and (2.36) using iterative method presented in Section 2.2.2, fault location and fault resistances can be estimated.

Pre-fault voltage at p_1, p_2, q_1 and q_2 can be estimated based on pre-fault node voltages and currents at the local substation. Approaches calculating node voltages and branch currents successively from the substation to the end of the feeder are proposed in [29], [61]. Method presented in [10] is adopted for determining the pre-fault voltage profiles, shown as follows:

$$[E_1] = [J_{11}][I_1] + [J_{1l}][I_l] \tag{2.37}$$

where

$[E_1]$ pre-fault voltages at local substation;

$[I_1]$ pre-fault currents at local substation;

$[I_l]$ pre-fault current injections by the remote source;

$[J]$ bus impedance matrix of pre-fault network excluding source impedances at local and remote substations;

$[J_{11}]$ submatrix of $[J]$ corresponding to the local substation;

$[J_{1l}]$ submatrix of $[J]$ corresponding to the transfer impedances between local and remote substations;

Rearranging (2.37), pre-fault current injections at remote substation can be acquired as:

$$[I_l] = [J_{1l}]^{-1}([E_1] - [J_{11}][I_1])$$ (2.38)

After pre-fault current injections at remote substation are determined, pre-fault voltages at all nodes can be determined. Current injection vector is composed of currents at local substation, currents at remote substation, and zero current injections at other nodes. The pre-fault voltages at all nodes are calculated as the product of bus impedance matrix $[J]$ and the current injection vector.

2.5 Fault Location Methods for Ungrounded Non-Radial Distribution Systems Using Line to Line Voltages and Line Currents

Sometimes, line to neutral measurements may not be available in reality. If so, fault location methods proposed in this section become an alternative when line to line voltages at local substation are available.

2.5.1 LL Faults

Consider an LL fault between phase 1 and 2, which could be any two phases out of phase A, B and C. Name the nodes corresponding to the faulted nodes at substation k_1 and k_2, respectively. The voltage change due to the fault from node k_1 to node k_2 is calculated as follows [57]:

$$\Delta E_{k_1 k_2} = E_{k_1 k_2} - E_{k_1 k_2 0} = -(Z_{k_1 r_1} - Z_{k_2 r_1})I_{f_1} - (Z_{k_1 r_2} - Z_{k_2 r_2})I_{f_2} \tag{2.39}$$

where

$E_{k_1 k_2}$ during-fault voltage from node k_1 to node k_2;

$E_{k_1 k_2 0}$ pre-fault voltage from node k_1 to node k_2;

$\Delta E_{k_1 k_2}$ voltage change from node k_1 to node k_2 due to the fault.

$$I_{f_1} = -I_{f_2} = \frac{(1-m)E_{p_1 p_2 0} + m E_{q_1 q_2 0}}{Z_{r_1 r_1} + Z_{r_2 r_2} - 2Z_{r_1 r_2} + R_{f_1}} \tag{2.40}$$

where $E_{p_1 p_2 0}$ is the pre-fault voltage from node p_1 to node p_2, $E_{q_1 q_2 0}$ is the pre-fault voltage from node q_1 to node q_2.

Equation used to estimate the unknown fault location and fault resistance is stated in (2.41).

$$\Delta E_{k_1 k_2} = [(1-m)E_{p_1 p_2 0} + m E_{q_1 q_2 0}]$$
$$\times \frac{[(B_{k_1 2} - B_{k_1 1} - B_{k_2 2} + B_{k_2 1}) + (C_{k_1 2} - C_{k_1 1} - C_{k_2 2} + C_{k_2 1})m]}{[(A_{11\_0} + A_{22\_0} - 2A_{12\_0}) + (A_{11\_1} + A_{22\_1} - 2A_{12\_1})m + (A_{11\_2} + A_{22\_2} - 2A_{12\_2})m^2 + R_{f_1}]} \tag{2.41}$$

By separating the above equation into real and imaginary parts, two real equations can be obtained, and then fault location and fault resistance can be estimated.

2.5.2 LLL Faults

For an LLL fault, the line to line voltage changes due to the fault at substation nodes can be expressed as

$$\Delta E_{k_1 k_2} = -(Z_{k_1 r_1} - Z_{k_2 r_1})I_{f_1} - (Z_{k_1 r_2} - Z_{k_2 r_2})I_{f_2} - (Z_{k_1 r_3} - Z_{k_2 r_3})I_{f_3} \qquad (2.42)$$

$$\Delta E_{k_1 k_3} = -(Z_{k_1 r_1} - Z_{k_3 r_1})I_{f_1} - (Z_{k_1 r_2} - Z_{k_3 r_2})I_{f_2} - (Z_{k_1 r_3} - Z_{k_3 r_3})I_{f_3}. \qquad (2.43)$$

Fault currents through fault resistances are given by (2.44) through the matrix form   [10].

$$\begin{bmatrix} I_{f_1} \\ I_{f_2} \\ I_{f_3} \end{bmatrix} = \begin{bmatrix} Z_{r_1 r_2} - Z_{r_1 r_1} - R_{f_1} & Z_{r_2 r_2} - Z_{r_1 r_2} + R_{f_2} & Z_{r_2 r_3} - Z_{r_1 r_3} \\ Z_{r_1 r_3} - Z_{r_1 r_1} - R_{f_1} & Z_{r_2 r_3} - Z_{r_1 r_2} & Z_{r_3 r_3} - Z_{r_1 r_3} + R_{f_3} \\ 1 & 1 & 1 \end{bmatrix}^{-1} \begin{bmatrix} -[(1-m)E_{p_1 p_2 0} + mE_{q_1 q_2 0}] \\ -[(1-m)E_{p_1 p_3 0} + mE_{q_1 q_3 0}] \\ 0 \end{bmatrix}$$

$$(2.44)$$

By defining the known variable vector X and obtaining function vector $f(X)$ based on (2.42) and (2.43), fault location and fault resistances can be obtained following the similar procedure as stated in Section 2.2.2.

2.6 Evaluation Studies

2.6.1 Fault Location Methods for Ungrounded Radial Distribution Systems

This section presents evaluation studies to verify the proposed fault location algorithms. MATLAB package SimPowerSystem is utilized to simulate the studied distribution

system [62]. Voltage and current waveforms under different fault types, fault locations and fault resistances are generated. A 16-bus, 12.47kV, 60Hz ungrounded radial distribution system, as shown in Figure 2.7, is utilized. Three-phase, two-phase laterals and loads are involved. A power factor of 0.9 lagging is assumed for all of the loads. Line length in miles, load ratings in kVA and load phases are labeled. Base values of 12.47kV and 1MVA are chosen for the per unit system.
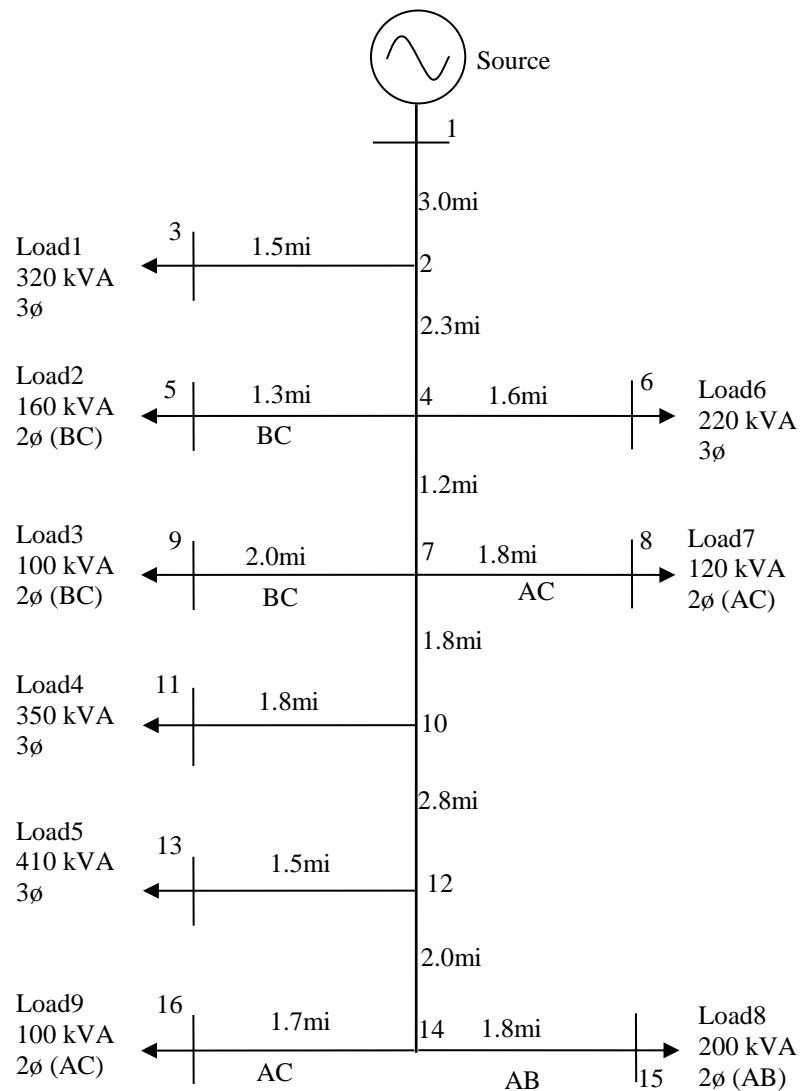
Figure 2.7 A sample ungrounded radial power distribution system

Source impedances for each generator in ohms and feeder impedance matrices in ohms/mile are given as follows, respectively [10], [63].

Source Impedances:

positive-sequence: $0.23 + j2.10$

zero-sequence: $0.15 + j1.47$

Main feeder impedance matrix:

[0.3465 + j1.0179   0.1560 + j0.5017   0.1580 + j0.4236

0.1560 + j0.5017   0.3375 + j1.0478   0.1535 + j0.3849

0.1580 + j0.4236   0.1535 + j0.3849   0.3414 + j1.0348].

Three-phase lateral feeder impedance matrix:

[0.7526 + j1.1814   0.1580 + j0.4236   0.1560 + j0.5017

0.1580 + j0.4236   0.7475 + j1.1983   0.1535 + j0.3849

0.1560 + j0.5017   0.1535 + j0.3849   0.7436 + j1.2112].

Two-phase lateral feeder impedance matrix:

[1.3294 + j1.3471   0.2066 + j0.4591

0.2066 + j0.4591   1.3238 + j1.3569].

The estimation accuracy of fault location is evaluated by the percentage error defined in (2.45).

$$\%\,Error = \left| \frac{Actual\ Location - Estimated\ Location}{Total\ Length\ of\ the\ Main\ Feeder} \right| \times 100. \qquad (2.45)$$

where the location of the fault is defined as the distance between the bus with lower index of the faulty line and the fault point. For example, if the fault occurs on line section between bus 1 and 2, the fault location is defined as the distance between bus 1 and the faulted point.

Fault location estimates are acquired by implementing the new algorithms in MATLAB. For algorithms requiring iterations, initial values of 0.5 per unit for fault location and 0.005 per unit for fault resistance are adopted. The tolerance of the biggest element in the unknown variable vector update is set to be 1×10^{-4}. In the evaluation studies, for estimates using iterative approaches, all solutions are acquired within 10 iterations.

Different evaluation studies have been carried out and results are presented in the rest of this section. The evaluation studies include fault location estimate accuracy analysis, impacts of load variation on fault location estimates, and sensitivity of fault location estimates to voltage and current errors.

Typical fault location results for cases with different fault types, fault locations and fault resistances are presented in Table 2.1 and Table 2.2. Table 2.1 shows fault location results using line to neutral voltages and line currents at the substation. The first four columns of Table 2.1 list the actual faulted section, fault type, fault location in per unit and fault resistance in ohms, respectively. Estimates of fault location errors in percentage and estimated fault resistances in ohms are listed in the last two columns. In Table 2.1, the LLL fault on line section 10-12 represents an unbalanced three-phase fault. Fault resistances [2, 4, 2] indicate that the three interphase fault resistances are $R_{f_1} = 2\Omega$,

$R_{f_2} = 4\Omega$, and $R_{f_3} = 2\Omega$, respectively. A fault location error of zero value indicates that

the error is less than 0.0005 in percentage.

Table 2.1 Fault Location Results Using Line to Neutral Voltages and Line Currents

Faulted section	Fault type	Fault location (per unit)	Fault resistance (ohm)	Fault location error (%)	Estimated fault resistance (ohm)
1-2	LL	0.3	5	0	5.002
	LLL	0.6	[1,1,1]	0.001	[1.001, 1.001, 1.001]
2-4	LL	0.4	8	0	8.002
	LLL	0.7	[10,10,10]	0.001	[10.001,10.001, 10.001]
4-5	LL	0.5	1	0.003	1.001
10-11	LL	0.6	10	0.002	10.002
	LLL	0.7	[5,5,5]	0.006	[5.001, 5.001, 5.001]
10-12	LL	0.2	2	0.002	2.003
	LLL	0.8	[2,4,2]	0.008	[2.001, 4.001, 2.001]
14-15	LL	0.4	5	0.001	5.002

Fault location results using line to line voltages and line currents at the substation

are displayed in Table 2.2.

It is evinced from Table 2.1 and 2.2 that highly accurate results have been

achieved by the proposed methods. The biggest fault location error occurs when using

line to neutral voltages and line currents at the substation with a LLL fault on line section

10-12. The error is 0.008%, which is still very small.

Table 2.2 Fault Location Results Using Line to Line Voltages and Line Currents

Faulted section	Fault type	Fault location (per unit)	Fault resistance (ohm)	Fault location error (%)	Estimated fault resistance (ohm)
1-2	LL	0.4	6	0	6.002
	LLL	0.8	[2,2,2]	0.002	[2.001, 2.001, 2.001]
2-3	LL	0.6	3	0	3.002
	LLL	0.7	[1,2,1]	0.002	[1.001, 2.001, 1.001]
4-7	LL	0.2	3	0	3.002
	LLL	0.3	[3,3,3]	0.004	[3.001, 3.001, 3.001]
7-8	LL	0.7	4	0.002	4.001
10-11	LL	0.7	5	0.003	5.002
	LLL	0.6	[2,2,2]	0.006	[2.001, 2.000, 2.001]
14-15	LL	0.8	7	0.001	7.002

Nominal equivalent load impedance is utilized to construct the bus impedance matrix in methods demonstrated in Sections 2.2 and 2.3. Therefore, actual load variations in the system may lead to errors in fault location estimation. The impacts of load variations on fault location estimates have been investigated in the study.

Table 2.3 presents four cases of individual load variations in percentage [10]. In the first two cases, load levels are decreased and increased by an average of 30%, respectively. In the last two cases, load levels are decreased and increased by an average of 20%, respectively.

Table 2.3 Individual load variations for ungrounded radial distribution systems

Case number	Load number								
	1	2	3	4	5	6	7	8	9
1	-40	-15	-25	-40	-20	-35	-40	-25	-30
2	40	15	25	40	20	35	40	25	30
3	-15	-25	-30	-10	-15	-25	-15	-30	-15
4	15	25	30	10	15	25	15	30	15

In order to mitigate the effects caused by load variations, the following method is adopted to compensate the load variations. Fault location methods based on line to line voltages and line currents at the substation are employed here. First, the load level under the prevailing operating condition is estimated based on the measured pre-fault voltages and currents at the substation. Then, based on the load level under the nominal condition and that under the prevailing operating condition, the equivalent load impedances are scaled as follows [12]:

$$S_{pwr} = (E_{k_1 0} - E_{k_3 0}) \times (I_{k_1 0})^* + (E_{k_2 0} - E_{k_3 0}) \times (I_{k_2 0})^* \qquad (2.46)$$

where S_{pwr} is the complex power injection to the substation preceding the fault and $*$ symbolizes complex conjugate operator. $E_{k_1 0}$, $E_{k_2 0}$ and $E_{k_3 0}$ are pre-fault voltages at the substation. $I_{k_1 0}$ and $I_{k_2 0}$ are pre-fault line currents flowing out of the substation. Node k_3 is chosen as the reference node here.

Then, the equivalent load impedances are scaled based on the following equation:

$$Z_{load\_new} = Z_{load} \times \frac{real(S_{pwr0})}{real(S_{pwr})} \tag{2.47}$$

where Z_{load_new} is the new load impedance, Z_{load} is the nominal load impedance, and S_{pwr0} is the power injection to the substation under nominal condition.

The newly obtained load impedances will then be utilized in the construction of the bus impedance matrix to reflect the load variations. Studies have shown that the load compensation technique is very effective. As an example, Table 2.4 and Table 2.5 present fault location errors before and after the mitigation for four cases of load variations given in Table 2.3. The first three columns of Table 2.4 and Table 2.5 present the actual fault type, fault location in per unit and fault resistance in ohm, respectively. Estimates of fault location errors in percentage before and after using mitigation methods are illustrated in the last four columns. All fault location results in these two tables are based on faults occurring on line section 10-12, which is a main feeder section.

Table 2.6 and Table 2.7 present fault location errors before and after using the load compensation method under the same four cases with fault occurring on a lateral feeder; line section 10-11. Fault location methods based on line to line voltages and line currents at the substation are also employed here. The first three columns of Table 2.6 and Table 2.7 show the actual fault type, fault location in per unit and fault resistance in ohm, respectively. Estimates of fault location errors in percentage before and after employing the mitigation methods are displayed in the last four columns.

Table 2.4 Load Compensation Results of Case 1 and 2 with fault occurring on line

section 10-12

Fault type	Fault location (per unit)	Fault resistance (ohm)	Fault location error (%)			
			Case 1		Case 2	
			Before Mitigation	After Mitigation	Before Mitigation	After Mitigation
LL	0.6	5	0.36	0.06	0.35	0.07
LL	0.3	2	0.24	0.05	0.24	0.06
LLL	0.2	[3,3,3]	0.29	0.08	0.28	0.07
LLL	0.7	[1,1,1]	0.44	0.09	0.41	0.08

Table 2.5 Load Compensation Results of Case 3 and 4 with fault occurring on line

section 10-12

Fault type	Fault location (per unit)	Fault resistance (ohm)	Fault location error (%)			
			Case 3		Case 4	
			Before Mitigation	After Mitigation	Before Mitigation	After Mitigation
LL	0.6	5	0.21	0.04	0.20	0.04
LL	0.3	2	0.12	0.00	0.12	0.01
LLL	0.2	[3,3,3]	0.15	0.02	0.14	0.01
LLL	0.7	[1,1,1]	0.24	0.03	0.21	0.01

Table 2.6 Load Compensation Results of Case 1 and 2 with fault occurring on line

section 10-11

Fault type	Fault location (per unit)	Fault resistance (ohm)	Fault location error (%)			
			Case 1		Case 2	
			Before Mitigation	After Mitigation	Before Mitigation	After Mitigation
LL	0.7	8	0.20	0.02	0.20	0.01
LL	0.4	2	0.20	0.03	0.19	0.04
LLL	0.3	[2,2,2]	0.25	0.05	0.24	0.05
LLL	0.8	[1,2,1]	0.40	0.05	0.38	0.06

Table 2.7 Load Compensation Results of Case 3 and 4 with fault occurring on line

section 10-11

Fault type	Fault location (per unit)	Fault resistance (ohm)	Fault location error (%)			
			Case 3		Case 4	
			Before Mitigation	After Mitigation	Before Mitigation	After Mitigation
LL	0.7	8	0.22	0.08	0.21	0.08
LL	0.4	2	0.11	0.01	0.11	0.02
LLL	0.3	[2,2,2]	0.14	0.07	0.13	0.01
LLL	0.8	[1,2,1]	0.24	0.04	0.22	0.03

As can be seen from Table 2.4 to 2.7, fault location accuracy has been greatly improved by utilizing the load compensation approach. Fault location error after mitigating the impacts of load variation is no larger than 0.09%. Fault location methods using line to neutral voltages yield very similar results.

The sensitivity of the developed methods to possible voltage and current measurement errors has also been examined. Scenarios with ± 1% and ± 2% errors assumed in voltage or current measurements have been studied. Impacts of voltage measurement errors on fault locations are presented in Table 2.8. Impacts of current measurement errors on fault locations are shown in Table 2.9. All fault location results in these two tables are based on faults occurring on line section 2-4.

Table 2.8 Impacts of voltage measurement errors on fault location estimates with fault occurring on line section 2-4

Fault type	Fault location (per unit)	Fault resistance (ohm)	Fault location error (%)			
			With -1% voltage error	With -2% voltage error	With 1% voltage error	With 2% voltage error
LL	0.3	5	0.28	0.56	0.28	0.56
LL	0.6	2	0.34	0.67	0.34	0.67
LLL	0.7	[3,3,3]	0.35	0.70	0.35	0.70
LLL	0.4	[2,1,3]	0.30	0.60	0.30	0.60

Table 2.9 Impacts of current measurement errors on fault location estimates with fault

occurring on line section 2-4

Fault type	Fault location (per unit)	Fault resistance (ohm)	Fault location error (%)			
			With -1% current error	With -2% current error	With 1% current error	With 2% current error
LL	0.3	5	0.28	0.57	0.28	0.55
LL	0.6	2	0.34	0.68	0.33	0.66
LLL	0.7	[3,3,3]	0.36	0.72	0.34	0.68
LLL	0.4	[2,1,3]	0.30	0.61	0.29	0.58

The first three columns of Table 2.8 and Table 2.9 give the actual fault type, fault location in per unit and fault resistance in ohm, respectively. Fault location errors in percentage with ± 1% and ± 2% errors in voltages or currents are presented in the last four columns. Fault location methods using line to line voltage measurements are utilized here.

From the above tables, it's demonstrated that for a ± 2% error in voltage measurement, fault location errors are within 0.70%, and for a ± 2% error in current measurement, fault location errors are within 0.72%.

Tables 2.8 to 2.9 have shown that the proposed fault location methods are insensitive to either voltage or current measurement errors.

2.6.2 Fault Location Methods for Ungrounded Non-Radial Distribution Systems
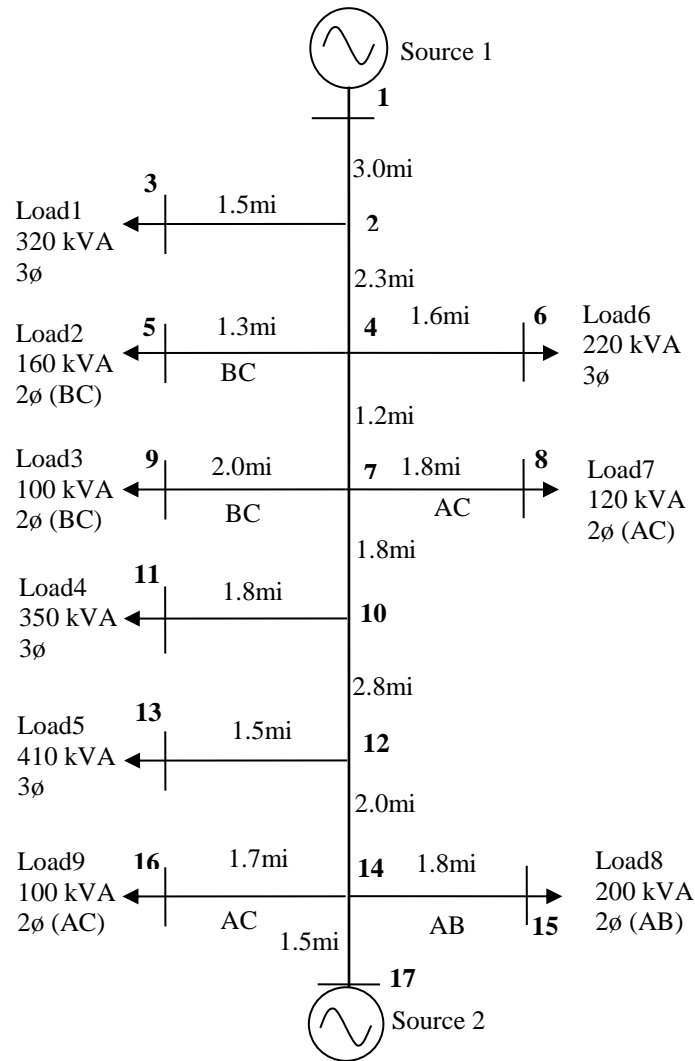
Figure 2.8 A sample ungrounded power distribution system

This section presents the evaluation studies to verify the proposed fault location algorithms. MATLAB package named SimPowerSystem is utilized to simulate the studied distribution system [62]. Voltage and current waveforms under different fault type, fault location and fault resistance are generated. Voltage and current phasors are extracted by using Fourier Transform. A 17-bus, 12.47kV, 60Hz ungrounded distribution

system, as shown in Figure 2.8, is utilized for the evaluation study. Three-phase, two-phase laterals and loads are involved. A power factor of 0.9 lagging is assumed for all of the loads. Line length in miles, load ratings in kVA and load phases are clearly labeled. Both Source 1 and Source 2 are in service. For convenience, base values of 12.47kV and 1MVA are chosen for the per unit system.

Fault location estimates are acquired by implementing the new algorithms in MATLAB [62]. The estimation accuracy of fault location is evaluated by the percentage error defined in (2.45). For algorithms using iterative approaches, initial values of 0.5 per unit for fault location and 0.005 per unit for fault resistances are adopted. The tolerance of the biggest element in the unknown variable vector update is set to be 1×10^{-4}. In the studies, for estimates using the iterative methods, all the estimations are obtained within 10 iterations.

Line parameters of the studied 17-bus system are the same as those of the ungrounded radial distribution system used in Section 2.6.1. Values of source impedances in ohms are demonstrated as below [10].

Source impedances of source 1:

positive-sequence: 0.23 + j2.10

zero-sequence: 0.15 + j1.47

Source impedances of source 2:

positive-sequence: 1.26 + j12.7

zero-sequence: 1.15 + j11.9

The rest of this section presents the fault location results under various studies, including fault location estimate accuracy analysis, impacts of load variation on fault location estimates, impacts of voltage and current errors on fault location estimates.

Typical fault location results on different line sections, under different fault types, fault locations and fault resistances are presented in Table 2.10 and Table 2.11.

Table 2.10 Fault location results using line to neutral voltages at local substation

Faulted section	Fault type	Fault location (per unit)	Fault resistance (ohm)	Fault location error (%)	Estimated fault resistance (ohm)
1-2	LL	0.2	5	0	5.002
	LLL	0.5	[2,2,2]	0	[2.001, 2.001, 2.001]
4-7	LL	0.3	10	0.001	10.001
	LLL	0.6	[5,5,5]	0	[5.000, 5.001, 5.001]
12-14	LL	0.7	2	0.004	2.001
	LLL	0.4	[4,4,4]	0.001	[4.000, 4.001, 4.001]
2-3	LL	0.8	10	0	10.001
	LLL	0.3	[2,4,6]	0	[2.001, 4.001, 6.000]
7-9	LL	0.5	1	0	1.002
14-15	LL	0.4	5	0	5.000

Table 2.10 shows the fault location results using line to neutral voltage measurements at local substation. The first four columns of Table 2.10 list the actual faulted section, fault type, fault location in per unit and fault resistance in ohms,

respectively. Estimates of fault location errors in percentage and estimated fault resistances in ohms are given in the last two columns. Fault location estimation error equals 0 indicates the error is less than 0.0005 in percentage.

Fault location results using line to line voltage data at local substation are displayed in Table 2.11.

Table 2.11 Fault location results using line to line voltages at local substation

Faulted section	Fault type	Fault location (per unit)	Fault resistance (ohm)	Fault location error (%)	Estimated fault resistance (ohm)
2-3	LL	0.1	3	0	3.002
	LLL	0.6	[2,3,3]	0	[2.001, 3.001, 3.001]
4-7	LL	0.2	10	0	10.001
	LLL	0.4	[1,1,1]	0	[1.001, 1.001, 1.001]
7-9	LL	0.6	4	0.001	4.002
7-10	LL	0.3	8	0.001	8.001
	LLL	0.3	[5,5,5]	0	[5.000, 5.001, 5.001]
12-14	LL	0.5	2	0.001	2.001
	LLL	0.2	[7,7,7]	0.001	[7.000, 7.001, 7.001]
14-16	LL	0.7	5	0.003	5.002

The biggest fault location estimate error is found when using line to line voltages at local substation with a LL fault on line section 12-14. The error is 0.004%. It is

evinced from Table 2.10 and 2.11 that highly accurate fault location estimates have been achieved by the proposed methods.

The fault location algorithms proposed in Section 2.4 and 2.5 uses equivalent impedance of load under nominal condition to build the bus impedance matrix. Consequently, load variation in the system may results in erroneous fault location. The influence of load variations on fault location estimates have been investigated in the study. Table 2.12 presents four cases of individual load variations in percentage [10]. Load levels are decreased by an average of 20% and 30% in the first two cases while load levels are increased by an average of 20% and 30% in the last two cases.

Table 2.12 Individual load variations for ungrounded distribution systems

Case	Load number								
number	1	2	3	4	5	6	7	8	9
1	-15	-25	-30	-10	-15	-25	-15	-30	-15
2	-40	-15	-25	-40	-20	-35	-40	-25	-30
3	15	25	30	10	15	25	15	30	15
4	40	15	25	40	20	35	40	25	30

In order to mitigate the effects caused by load variation, the following method is adopted to compensate the load variation.

First, the load level under the prevailing operating condition is estimated by using Equation (2.46). Pre-fault voltage and current measurements at the local substation are involved. Then, Equation (2.47) is adopted to scale the load impedance based on the load level under the nominal condition and that under the prevailing operating condition.

Table 2.13 and Table 2.14 reveal the effectiveness of the load compensation technique. Table 2.13 presents fault location estimates before and after the mitigation process under case 1 and case 2 of load variation. Table 2.14 lists fault location estimates before and after mitigation process under case 3 and case 4 of load variation. For both tables, faults occur on line section 7-10. The first three columns of Table 2.13 and Table 2.14 give the actual fault type, fault location in per unit and fault resistance in ohm, respectively. Estimates of fault location errors in percentage before and after using mitigation methods are listed in the last four columns. Fault location methods based on line to line voltages are employed here. Fault location methods using line to neutral voltages yield similar results.

Table 2.13 Impacts of load compensation of case 1 and 2 with fault occurring on line section 7-10

Fault type	Fault location (per unit)	Fault resistance (ohm)	Fault location error (%)			
			Case 1		Case 2	
			Before Mitigation	After Mitigation	Before Mitigation	After Mitigation
LL	0.7	5	0.36	0.03	0.62	0.04
LL	0.2	2	0.16	0.01	0.28	0.02
LLL	0.3	[3,3,3]	0.39	0.02	0.65	0.03
LLL	0.6	[1,1,1]	0.20	0.02	0.34	0.02

Table 2.14 Impacts of load compensation of case 3 and 4 with fault occurring on line

section 7-10

Fault type	Fault location (per unit)	Fault resistance (ohm)	Fault location error (%)			
			Case 3		Case 4	
			Before Mitigation	After Mitigation	Before Mitigation	After Mitigation
LL	0.7	5	0.36	0.03	0.61	0.05
LL	0.2	2	0.15	0.01	0.27	0.03
LLL	0.3	[3,3,3]	0.38	0.03	0.64	0.05
LLL	0.6	[1,1,1]	0.20	0.02	0.33	0.03

Table 2.15 and Table 2.16 present fault location errors before and after utilizing the load compensation method under four cases with fault occurring on a three-phase lateral feeder section; section 12-13. Fault location methods based on line to line voltages are also employed in this study. The first three columns of Table 2.15 and 2.16 display the actual fault type, fault location in per unit and fault resistance in ohm, respectively. Estimates of fault location errors in percentage before and after using mitigation methods are listed in the last four columns.

Table 2.15 Impacts of load compensation of case 1 and 2 with fault occurring on line

section 12-13

Fault type	Fault location (per unit)	Fault resistance (ohm)	Fault location error (%)			
			Case 1		Case 2	
			Before Mitigation	After Mitigation	Before Mitigation	After Mitigation
LL	0.5	3	0.24	0.02	0.42	0.03
LL	0.8	8	0.45	0.03	0.74	0.03
LLL	0.4	[3,3,5]	0.40	0.01	0.71	0.04
LLL	0.7	[2,2,2]	0.34	0.02	0.58	0.03

Table 2.16 Impacts of load compensation of case 3 and 4 with fault occurring on line

section 12-13

Fault type	Fault location (per unit)	Fault resistance (ohm)	Fault location error (%)			
			Case 3		Case 4	
			Before Mitigation	After Mitigation	Before Mitigation	After Mitigation
LL	0.5	3	0.24	0.02	0.42	0.05
LL	0.8	8	0.43	0.03	0.73	0.06
LLL	0.4	[3,3,5]	0.40	0.02	0.70	0.06
LLL	0.7	[2,2,2]	0.33	0.02	0.57	0.05

As can be seen from these two tables, fault location accuracy has been greatly improved with the load compensation approach. Fault location error after alleviate the impacts of load variation is no larger than 0.06%.

The sensitivity of the developed methods to measurement errors has also been examined. Table 2.17 shows the estimated fault location errors for faults on line section 4-7 with 1% and 2% errors assumed in pre-fault voltage measurements. Impacts of pre-fault current measurement errors are shown in Table 2.18. The first three columns of Table 2.17 and Table 2.18 give the actual fault type, fault location in per unit and fault resistance in ohm, respectively. Fault location errors with $\pm$ 1% and $\pm$ 2% errors in voltages or currents are presented in the last four columns.

Table 2.17 Impacts of measurement errors in voltages on fault location estimates with

fault occurring on line section 4-7

Fault type	Fault location (per unit)	Fault resistance (ohm)	Fault location error (%)			
			With -1% voltage error	With -2% voltage error	With 1% voltage error	With 2% voltage error
LL	0.2	5	0.04	0.15	0.04	0.18
LL	0.3	2	0.71	1.43	0.72	1.43
LLL	0.3	[1,3,2]	0.48	1.00	0.44	0.85
LLL	0.7	[4,4,4]	0.68	1.15	0.93	2.13

Table 2.18 Impacts of measurement errors in currents on fault location estimates with

fault occurring on line section 4-7

Fault type	Fault location (per unit)	Fault resistance (ohm)	Fault location error (%)			
			With -1% current error	With -2% current error	With 1% current error	With 2% current error
LL	0.2	5	0.02	0.05	0.02	0.05
LL	0.3	2	0.02	0.04	0.02	0.04
LLL	0.3	[1,3,2]	0.02	0.05	0.02	0.05
LLL	0.7	[4,4,4]	0.03	0.07	0.03	0.07

From the above tables, it's demonstrated that for a ± 2% error in pre-fault voltage measurement, fault location errors are within 2.13%, and for a ± 2% error in pre-fault current measurement, fault location errors are within 0.07%. In fault location methods proposed in Section 2.4 and 2.5, pre-fault voltages at all nodes are calculated based on the pre-fault currents at the local and remote substations. Therefore, erroneous pre-fault currents will lead to incorrect pre-fault voltages at the ends of the faulted line, which results in incorrect fault location estimates.

Fault location methods using line to line voltage measurements are utilized here. Fault location methods using line to neutral voltages generate similarly robust results.

2.7 Summary

Novel fault location algorithms for both ungrounded radial and non-radial distribution systems have been presented in this Chapter. Methods using either line to neutral voltages or line to line voltages are proposed and evaluated for both types of distribution systems.

The proposed fault location methods for radial ungrounded systems utilize only during-fault voltage and current measurements at the substation. However, pre-fault data are harnessed to effectively mitigate impacts of load variations. The proposed algorithms are independent of source impedance, and an approach has been presented for the construction of bus impedance matrix excluding source impedance.

Fault location methods for non-radial ungrounded distribution systems eliminate or reduce the need for iterative procedures and yield accurate results.

The network topology change has impacts on fault location accuracy, as on all existing fault location algorithms. It's envisioned that the proposed methods can be implemented as real time online fault location methods. In order to ensure the accuracy of fault location estimates, network configuration should be updated timely based on available real time grid monitoring information. An algorithm used for monitoring network topology changes is referred to [64]. If the network topology changes, the related information will be transferred to the fault location module for enhanced fault location accuracy.

Last but not the least, evaluation studies have demonstrated that the proposed methods produce accurate fault location estimates, and are robust to load variations and measurement errors.

Chapter 3   Distribution System Fault Location Observability Studies and Optimal Meter Placement

An optimal meter placement scheme for transmission line has been proposed in [48]. Chapter 3 extends the idea to distribution systems. This chapter is organized as follows. Section 3.1 presents a brief introduction about this section. Section 3.2 describes how to perform fault location observability analysis. Algorithm of optimal meter placement for fault location is discussed in Section 3.3. Case studies on a sample power distribution system are reported in Section 3.4. Conclusions are made in Section 3.5.

3.1   Introduction

Most of the fault location methods developed in the past employ measurements obtained from a limited number of meters installed in a power system. Optimal meter placement in power systems is to make the best use of a limited number of meters available to keep the entire network observable. This section presents fault location observability analysis for distribution systems, and proposes a novel optimal meter placement algorithm to keep the system observable in terms of fault location determination. First, the observability of fault location in power systems is defined. Then analysis of the whole system is performed to determine the least number of meters needed and the best locations to place those meters in order to achieve fault location observability. Case studies based on a 16-bus distribution system have been carried out to illustrate the proposed algorithms.

3.2   Fault Location Observability Analysis

The definition of location observability is illustrated by taking a three-bus sample power system as an example, as shown in Figure 3.1. In this system, there are three buses and

three possible fault locations F_1, F_2 and F_3. If two different fault locations F_1 and F_2 yield the same measurements at a bus, say bus 1, the two fault locations will be indistinguishable based solely on the measurements at bus 1. In this case, fault locations F_1 and F_2 are called unobservable. On the contrary, if a unique fault location, say F_1, can be deduced based on the measurements at bus 1, and then location F_1 is called observable with the measurements from bus 1. A meter at bus 1 is needed to make location F_1 observable.
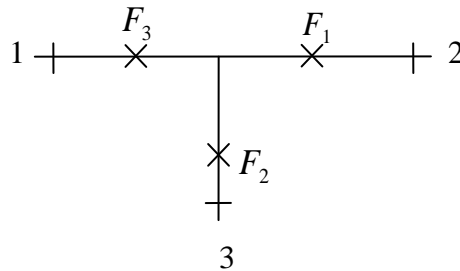
Figure 3.1 A sample three-bus power system

In another example, if two possible fault locations F_1 and F_2 can be derived from the measurements at bus 1, and two possible fault locations F_1 and F_3 can be obtained from the measurements at bus 3. Then the combination of measurements from bus 1 and bus 3 can lead to the unique fault location F_1. Under this circumstance, fault location F_1 is called observable with the measurements from bus 1 and 3. Meters at bus 1 and 3 are needed to make location F_1 observable.

In order to examine the fault location observability of a network, a fault location method is needed to estimate the fault location. Any fault location method can be utilized to perform the fault location observability analysis as long as the type of installed meters can provide the measurements required for fault location. In this dissertation, a previously

proposed fault location method using measurements at a single bus is adopted to perform the observability analysis [10], which will be reviewed in Section 3.4.

The procedure to determine the observability of a fault location is described as follows. Suppose that a meter is placed at bus k in the power system. First, suppose that a specific fault, say an LG fault with a fault resistance of 1 ohm, is posed on a line at location F_1. Based on the short-circuit analysis, the during-fault measurements at bus k can be calculated. With the measurements at bus k, the adopted fault location method is then applied to each line section of the power system, and a set of possible fault locations on different line sections are obtained, denoted as set S_k. If set S_k contains only one fault location, which means fault location F_1 can be uniquely determined based on voltage measurements at bus k, fault location F_1 is regarded as observable. If set S_k contains more than one fault location, it indicates that fault location F_1 is not observable with the measurements at bus k.

To make fault location F_1 observable, more meters are needed. Now assume that another meter is placed at another bus, say bus l. Similarly, the voltage measurements at bus l can be utilized to acquire the corresponding set of possible fault locations S_l. The intersection of S_k and S_l, denoted as $S_{k,l}$, gives the most likely fault locations based on the voltage measurements at bus k and l. If set $S_{k,l}$ contains only one fault location, the fault point F_1 can be uniquely determined based on the voltage measurements at bus k and l, and fault location F_1 is said to become observable. Otherwise, the voltage measurements at bus k and l are still inadequate to uniquely determine the fault location F_1.

Fault location observability can be analyzed similarly for the circumstances where there are more than two meters installed in a power system.

Generally speaking, if any two different fault locations can be distinguished from each other by using the available measurements, the system is said to be observable. If one fault location cannot be distinguished from another fault location with the available measurements, this fault location is called an unobservable point.

To study the observability of the entire power system, each line of the system is truncated into short segments of equal length. For instance, if a 2-mile line is truncated with a resolution of 0.2 mile, 10 segments can be acquired with 11 separate points. By examining the observability of these 11 points, the observability of this line can be studied. With the observability of each line in the system being analyzed, the observability of the entire power system can be determined. If there is any unobservable point in the system, the system is not observable.

If a meter is available at each bus, then the system will certainly be observable. It would be desirable to find out the least costly scheme or the minimum number of meters required keeping the system observable, which is discussed in the following section.

3.3 Optimal Meter Placement Method

To solve the optimal meter placement problem is to find out the optimal locations for meters to be placed in a system so as to make the entire system observable while the total cost or the number of meters needed is minimized.

The optimal meter placement problem is formulated as an integer linear programming problem as follows [48].

The optimal meter placement problem can be solved by minimizing the objective function

$$J = \sum_{i=1}^{n} c_i M_i \qquad (3.1)$$

subject to a set of linear constraints, where c_i represents the monitoring cost for a meter installed at bus i. The value of $M_i, i = 1,...,n$ indicates if a meter is placed at bus i or not. $M_i = 1$ represents a meter is placed at bus i and $M_i = 0$ represents no meter is placed at bus i.

As mentioned in Section 3.2, the fault location observability of the whole power system is decided by examining the fault location observability of different points in a distribution system. For each point under certain fault type and fault resistance, a set of linear constraints can be derived to make this specific fault location observable. To make the entire power system fully observable, the linear constraints for each fault location under all fault types and varying fault resistances should be satisfied. Therefore, by minimizing the value of objective function J subject to all constraints obtained, the optimal solution can be determined.

The procedure to construct the constraints is illustrated by taking a fault location F_1 as an example. First, assume that a fault occurs at location F_1, based on which measurements at each bus can be obtained through short-circuit analysis. Then, with measurements at bus $i, i = 1,...,n$, a set of possible fault locations, say $S_i, i = 1,...,n$, can be acquired by applying the employed fault location method to each line of the power system. As a result, a total number of n sets can be obtained. Then, the bus

54

number/numbers, whose voltage and current measurements will make F_1 observable, are identified and recorded as follows. First, identify the set with only one element. If set S_{i_1} has only one element, it indicates that the measurements at bus i_1 can uniquely determine the fault location F_1. The bus number is recorded as $\{i_1\}$. Then, for fault location sets with two or more elements, obtain the intersection of any two sets, say S_{i_2} and S_{i_3}. If the intersection S_{i_2,i_3} contains one element, it can be inferred that measurements at bus i_2 and i_3 are sufficient to uniquely pinpoint the fault location F_1. Record the bus numbers $\{i_2, i_3\}$. If the combination of two sets is not enough to uniquely determine fault location F_1, another set can be added to see if the fault location F_1 can be uniquely determined. In this way, all possible sets of meters to make F_1 observable can be identified.

Based on all the obtained sets with recorded bus number/numbers, the constraints of the optimization problem are then constructed. An example is provided here to explain the procedure. Suppose that there is a four-bus power system, with buses numbered 1, 2, 3 and 4. For a studied fault location, by applying the above method to the system, three sets of buses are yielded: {1, 2}, {1, 3}, {4}. It indicates that if there are meters at buses 1 and 2, or at buses 1 and 3, or solely at bus 4, the studied fault location can be uniquely determined. Based on the definition of M_i $(i = 1,...,n)$, the above statement can be represented by the following constraint:

$$(M_1 \text{ AND } M_2) + (M_1 \text{ AND } M_3) + M_4 \geq 1 \qquad (3.2)$$

where AND represents the logical AND operator.

Equation (3.2) can be transformed to linear constraints as shown in [48].

To make a power system fully observable, one should first derive the constraints corresponding to a certain fault location under a specified type of fault and fault resistance. Then constraints for all the other fault locations and resistances under the same fault type can be acquired similarly. In the end, one can derive the constraints for all fault locations under all types of faults and fault resistances. By minimizing the objective function subject to all of the constraints, the optimal meter placement problem can be solved.

3.4 Fault Location Methods

In this section, a previously proposed fault location method using measurements at a single bus is reviewed, and utilized to perform the observability analysis.

The proposed fault location methods for LG, LL, LLG, LLL and LLLG faults have been derived respectively, as can be referred to [10]. Fault location approaches for LG will be illustrated here as an example. Methods for other types of faults can be found in [10]. The same notations used in Section 2.1.2 are utilized here for consistency. However, it should be noted that in this chapter, k_1, k_2 and k_3 represents nodes corresponding to the faulted phases at the bus with a meter. They no longer present the nodes corresponding to the faulted phases at the substation. Figure 3.2 depicts the diagram of LG, LLG and LLLG faults, where fictitious nodes representing the fault points on the faulty line are named r_1, r_2, and r_3, respectively. Figure 2.2 demonstrate a fault occurring on a three-phase line section with fictitious nodes drawn on each phase. The construction of bus impedance matrix can be referred to descriptions in Section 2.1.3.

In this study, an LLL or an LLLG fault can either be a balanced fault or an unbalanced fault.
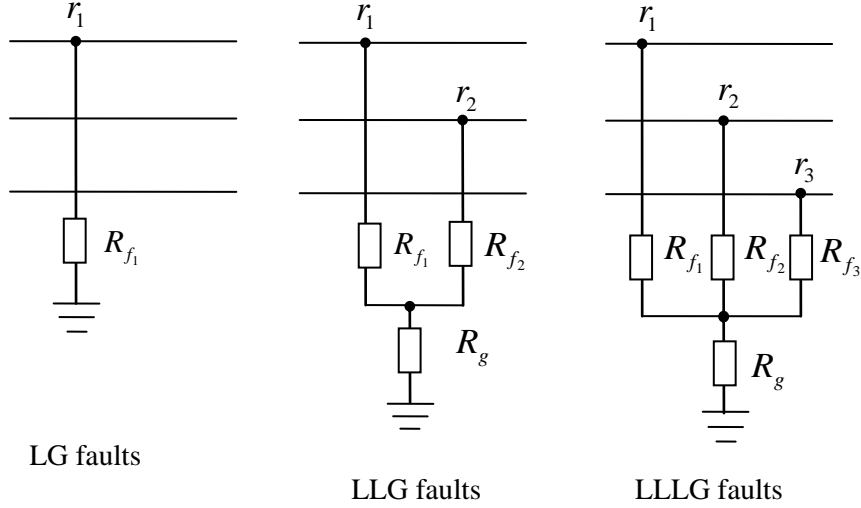
Figure 3.2 Diagrams of LG, LLG and LLLG faults

3.4.1 LG Faults

For an LG fault with the faulted phase being phase A, B, or C, designate the node corresponding to the faulted phase at the bus with a meter as k_1. The voltage change due to the fault at node k_1, or superimposed voltage at node k_1, is calculated as [10]:

$$\Delta E_{k_1} = E_{k_1} - E_{k_1 0} = -Z_{k_1 r_1} I_{f_1} \tag{3.3}$$

where

E_{k_i} during-fault voltage at node k_i;

$E_{k_i 0}$ pre-fault voltage at node k_i;

ΔE_{k_i} voltage change at node k_i due to the fault;

57

I_{f_i} fault current flowing through the fault resistance out of the fault node r_i. It's negative of current injection.

Fault current can be obtained by the following form [58], [60]:

$$I_{f_1} = \frac{E_{r_1 0}}{Z_{r_1 r_1} + R_{f_1}}$$ (3.4)

where

R_{f_1} fault resistance between node r_1 and the ground.

From Figure 2.2, pre-fault voltage at fault node r_1 can be acquired as shown in (2.31). $E_{p_1 0}$ and $E_{q_1 0}$ can be determined after pre-fault voltage profile is obtained following the procedure described in Section 2.4.2.

Substituting (2.31) and (3.4) into (3.3), the following equation is yielded for estimating the unknown fault location.

$$\Delta E_{k_i} = \frac{-E_{p_1 0} + m(E_{p_1 0} - E_{q_1 0})}{A_{11\_0} + A_{11\_1}m + A_{11\_2}m^2 + R_{f_1}}(B_{k_i 1} + C_{k_i 1}m)$$ (3.5)

where $B_{k_1 i}, C_{k_1 i}, A_{it\_0}, A_{it\_1}, A_{it\_2}, A_{ii\_0}, A_{ii\_1}, A_{ii\_2} (i = 1,2,3)$ are constants given in Section 2.1.2, which are determined by the network parameters.

By separating (3.5) into real and imaginary parts, two real equations can be obtained, from which the fault location m can be estimated.

For LLG, LLL and LLLG faults, one should choose suitable unknown variable vector X and construct related function vector $F(X)$. Then, fault location can be estimated using the iterative method discussed in Section 2.2.2.

By applying the above fault location method to each line section of the system, a list of likely fault location estimates may be generated, comprising the true estimate and the fake estimates. Depending on available measurements, some of the fake estimates may be eliminated as illustrated in Section 3.5.1, while other fake estimates may be indistinguishable from the true fault location.

3.5 Evaluations studies
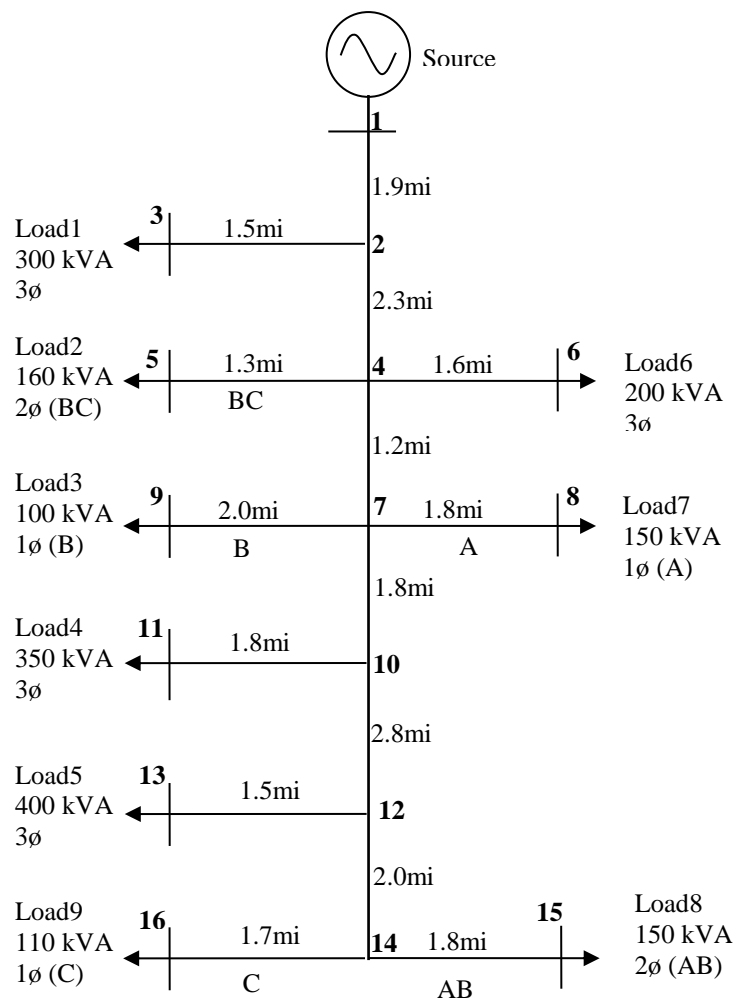
Figure 3.3 A sample power distribution system

This section presents the case studies and results of the proposed methods for performing fault location observability analysis and optimal meter placement. A 16-bus, 12.47kV, 60Hz distribution system, as shown in Figure 3.3, is utilized for the study, with detailed system parameters referred to [63]. The system is a typical distribution system including unbalanced lateral feeders and loads of single-phase, two-phase or three-phase. A lagging power factor of 0.9 is assumed for all the loads. Line length in miles, load ratings in kVA and load phases are labelled. A resolution of 0.2 mile is used for studying fault location observability. Base values of 12.47kV and 1MVA are selected for the per unit system.

Studies for faults with different types including LG, LL, LLG, LLL, LLLG faults have been carried out. For ground faults, fault resistances of 1, 50, 100 ohms are used. For other fault types, fault resistances of 1 and 5 ohms are employed.

In the following sections, a method to reduce or eliminate multiple possible fault location estimates to reach a unique estimate is first discussed in Section 3.5.1. Then, Section 3.5.2 presents the fault location observability analysis results. The optimal meter placement results are reported in Section 3.5.3.

3.5.1 Method to Trim Multiple Fault Location Estimates

As mentioned in Section 3.2, for a specific fault, with voltage measurements available at one given bus, several possible fault locations on different lines may be acquired. Except the actual fault location, other fault locations are called fake fault locations. The following example illustrates why fake fault locations exist. Suppose that an AG fault with a 1 ohm fault resistance is posed at 1.2 miles away from bus 7 on line section 7-8 in the system. Voltages at bus 7 are considered as known measurements. By using the measurements, four fault location estimates are obtained as presented in Table 3.1.

Table 3.1 Fake fault location analysis results under an AG fault with a 1-ohm fault

resistance on line section 7-8

Fault location Number	Estimated fault location (mile)	Voltage difference between measured and calculated voltage at bus 7 (per unit)
1	[2, 3, 0.67]	{0, 0.1055, 0.0938}
2	[4, 6, 1.07]	{0, 0.0232, 0.0207}
3	[7, 8, 1.20]	{0, 0, 0}
4	[7, 10, 1.49]	{0, 0.0037, 0.0037}

The significance of Table 3.1 is explained below.

In order to closely examine these four fault locations, the following procedure is performed to analyze each fault location estimate.

1.   Assume a fault does occur at the estimated fault location.

2.   Perform short-circuit analysis to calculate the during-fault voltages at the bus providing measured voltages, which is bus 7 in this case. The voltages calculated in this step are designated as calculated voltages, which are used to be compared with the measured voltages employed to calculate the fault location estimate.

3.   Compare the measured and calculated voltages at the bus with the measured voltages, i.e., bus 7.

Table 3.1 shows the results of above analysis on the four estimated fault locations. The first, second and third columns list the fault location number, estimated fault location in miles, and per unit voltage differences between the measured and calculated during-fault voltages in three phases. Fault location 1 - [2, 3, 0.67] represents a fault at 0.67 miles away from bus 2 on line section 2-3. {0, 0.1055, 0.0938} denotes the differences between the measured and calculated voltages in per unit at bus 7 for phase A, B and C, respectively. Other fault location estimates in Table 3.1 can be interpreted similarly. The third fault location estimate is the true value and the other three locations are fake estimates.

Table 3.1 manifests that all the four fault location estimates have the same calculated phase A voltage at bus 7, which is expected. This is because the fault location method utilized only during-fault phase A voltage for an AG fault, and phase B and C voltages are not used. Thus, comparison of the measured voltages with the calculated ones may help identify certain fake fault locations as follows.

For a fault location estimate, if the calculated voltages are different from the measured voltages, this fault location is considered as a fake one. In this chapter, a tolerance of 0.01 per unit is adopted to judge whether two values are different or not, with consideration of potential measurement errors. According to this criterion, in Table 3.1, fault locations 1 and 2 are identified as fake locations. Fault location 4 is indistinguishable from the true fault location using only the voltage measurements. So, not all fake fault locations can be identified.

When available, measured line currents will be adopted to further reduce the number of fake fault locations. For a fault location estimate F_1 with measurements

available from bus k, if the calculated voltages and currents at bus k are different from measured voltages and currents at bus k, this fault location is a fake one. To simplify the procedure, the problem of comparing a branch current is transformed into comparing the voltages at both ends of the branch. A tolerance of 0.01 per unit is used.

Another example is provided below to further elucidate that utilizing both voltages and currents will help eliminate fake estimates. Table 3.2 gives fault location estimates with measurements available at bus 10. A BG fault with a fault resistance of 50 ohms occurs at 0.7 miles away from bus 7 on line section 7-10. In Table 3.2, the first column lists the case number, and the second column displays the estimated fault locations. Case 1 represents the circumstances where only voltage measurements are utilized to calculate the fault location and no fake fault locations are eliminated. In case 2, fake fault locations are removed by comparing calculated voltages based on estimated fault location with measured voltages at bus 10. In case 3, fake fault locations are eliminated by comparing calculated measurements, including both voltages and currents, with measured measurements at bus 10. Since a meter is installed at bus 10, current flowing from bus 10 to 7, 10 to 11 and 10 to 12 are assumed to be known. All these three branch currents are used to determine the fake fault locations in case 3.

It can be seen from Table 3.2, that five possible fault locations are acquired in case 1 with measurements at bus 10. In case 2, by comparing the calculated and measured voltages at bus 10, fault location [2, 3, 1.24] has been detected as a fake fault location, and removed from fault location list. In case 3, three more fault locations are removed when compared to case 2. Only the actual fault location is left. It's evinced that some

63

fake fault locations can be eliminated by taking advantage of both voltages and currents at the bus with measurements.

Table 3.2 Fault location results under three different cases under a BG fault with a 50-ohm fault resistance on line section 7-10

Case Number	Estimated fault location (mile)
1	[2, 3, 1.24]
	[4, 5, 0.42]
	[4, 6, 0.49]
	[7, 9, 0.24]
	[7, 10, 0.70]
2	[4, 5, 0.42]
	[4, 6, 0.49]
	[7, 9, 0.24]
	[7, 10, 0.70]
3	[7, 10, 0.70]

In the following sections, both voltage and current measurements are utilized to eliminate fake fault locations. It will be shown that to eliminate all the fake fault location estimates, it may be necessary to install more meters in the system.

3.5.2 Fault Location Observability Analysis Results

In the study, if the difference between two calculated possible fault locations is less than 0.01 mile, the two fault locations will be considered to be the same estimate. This criterion helps to determine whether a fault location exists in the intersection of two fault

location sets discussed in Section 3.2. Representative observability study results are shown as follows.
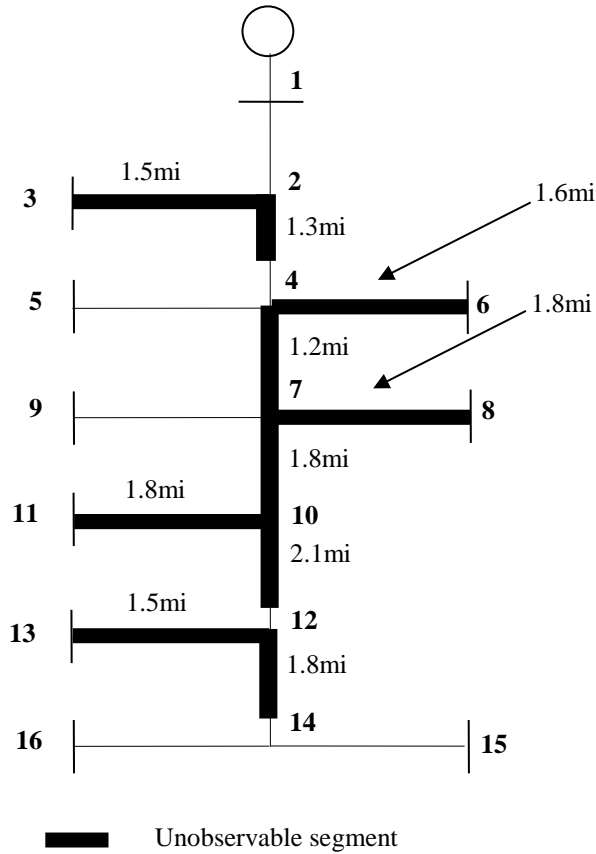
Figure 3.4 Unobservable segments under AG faults with a 50-ohm fault resistance with a meter placed at bus 1

Suppose that only one meter is placed at bus 1 and voltages and currents at bus 1 are measured. The fault location observability analysis has been performed. Figure 3.4 depicts the analysis results for AG faults with a fault resistance of 50 ohms. The unobservable segments of the studied system are marked with black rectangles, with the length of each unobservable segment being labelled. Remaining segments are observable. Please notice AG fault is not applicable to line 4-5, 7-9, or 14-16, since these lines do not

have phase A. From Figure 3.4, it is shown that many of the lines are unobservable if there is only one meter placed at bus 1.
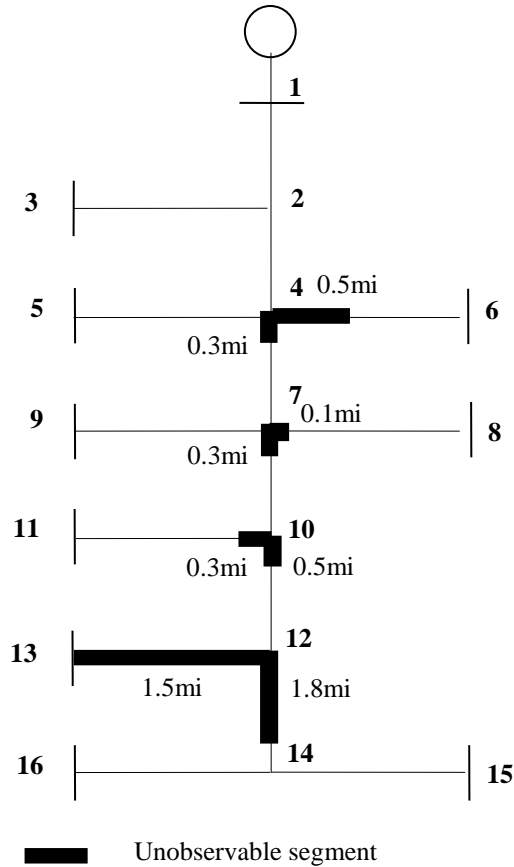
Figure 3.5 Unobservable segments under AG faults with a 50-ohm fault resistance with meters placed at buses 1 and 3

Figure 3.5 shows unobservable segments under AG faults with a 50-ohm fault resistance after another meter is placed at bus 3. It demonstrates that the unobservable segments have been significantly reduced after adding a meter to the system.

To further explicate the impact of the number of measurements on fault location observability, Table 3.3 presents estimated fault locations under BG faults with a 1-ohm fault resistance under different meter placements. The first column gives the actual fault

location. The second and third columns list the estimated fault locations using measurements at buses 5 and 6, respectively. The last column presents the estimated fault locations with meters placed at both buses 5 and 6. For fault location [2, 3, 0.30], a meter at bus 5 or bus 6 alone is enough to make this fault location observable. For the fault location of 0.2 miles from bus 4 to 7, employing measurements at bus 5, two possible fault locations can be calculated: one being 0.25 miles from bus 4 to 6, and the other being 0.20 miles from bus 4 to 7. Utilizing measurements at bus 6 alone also yields two estimates. The combination of measurements at buses 5 and 6 leads to a unique fault location, which is 0.20 miles from bus 4 to 7. So, meters at both buses 5 and 6 are needed to make this fault location observable. For the third fault location, meters at buses 5 and 6 are insufficient to make the fault location observable.

Table 3.3 Fault location set under BG faults with a 1-ohm fault resistance

Actual Fault location (mile)	Estimated fault location (mile) /Bus 5	Estimated fault location (mile) / Bus 6	Estimated fault location (mile) / Bus 5 and 6
[2, 3, 0.3]	[2, 3, 0.30]	[2, 3, 0.30]	[2, 3, 0.30]
[4, 7, 0.2]	[4, 6, 0.25] [4, 7, 0.20]	[4, 5, 0.20] [4, 7, 0.20]	[4, 7, 0.20]
[12, 14, 0.3]	[12, 13, 0.23] [12, 14, 0.30]	[12, 13, 0.23] [12, 14, 0.30]	[12, 13, 0.23] [12, 14, 0.30]

3.5.3 Optimal Meter Placement Analysis

As presented in Section 3.3, the optimal meter placement problem is formulated as an integer linear programming problem. Observability studies have been performed for LG, LLG, and LLLG faults with fault resistances vary from 1 to 100 ohms, and LL, LLL faults with fault resistances varying from 1 to 5 ohms. Constraints for each type of faults are obtained. Then, the linear programming problem is constructed with those constraints, and is solved by using IBM ILOG CPLEX package.

Table 3.4 Optimal meter placement solutions with equal monitoring costs at each

location

Fault type	Minimum number of meters needed	Optimal meter locations
LG	4	{1, 3, 6, 14}
LL	3	{1, 5, 13};{1, 5, 14};{1, 5, 15}; {1, 6, 13};{1, 6, 14};{1, 6, 15}
LLG	3	{1, 4, 14};{1, 5, 14};{1, 6, 14}
LLL	2	{1, 13};{1, 14}
LLLG	2	{1, 13};{1, 14}
LG, LL, LLG, LLL, LLLG	4	{1, 3, 6, 14}

Table 3.4 lists the meter placement results under different fault types with an equal monitoring cost for each monitoring location. The first column of Table 3.4 gives

the fault type. The second column lists the minimum number of meters that are needed. Optimal meter locations are presented in the last column.

In this study, it is assumed that a meter is always placed at substation (bus 1), which is usually the case in practice. As a result, meter placement results for each fault type have a "1" in meter location set. It's demonstrated that four meters are needed to make the system observable for LG faults, three meters are required for LL and LLG fault, and only two meters are enough to uniquely locate any LLL or LLLG faults. The last row indicates that, to make the system observable under all types of fault, at least four meters are needed to be deployed at bus 1, 3, 6, and 14, respectively.

It should be noticed that the optimal meter placement yields the least number of meters and the locations to place the meters so as to make the system observable. Therefore, any meter placement set that contains the optimal meter set also has the ability to make the system observable. For example, a set of meters at bus {1, 5, 13} can uniquely determine any LL fault, then a set of meters at bus {1, 5, 13, k } $(k = 1,...,16 \text{ and } k \neq 1,5,13)$ can definitely pinpoint any LL fault uniquely. Besides, multiple optimal meter placements may exist for some fault types. For instance, according to Table 3.4, there are six optimal solutions for LL faults.

Sometimes, the monitoring expenses at different locations may not be the same. It may be easier to install a meter at a certain location, and therefore the monitoring cost will be lower at this location. Or, if a meter is needed at a location for multiple purposes such as fault location and power quality monitoring, the monitoring cost for this location will be lower to represent a higher need. Different monitoring costs will impact the optimal meter placement solution as shown below.

Table 3.5 shows the optimal meter placement results for LL faults under different monitoring cost distributions. The first column indicates the case number. The second column presents the monitoring costs at each location. The third and fourth columns list the minimum number of meters needed and their locations.

Table 3.5 Optimal meter placement solutions for LL faults with varying monitoring coasts at each location

Case number	Monitoring costs	Minimum number of meters needed	Optimal meter locations
1	c_i is equal for $i = 1,...,16$	3	{1, 5, 13};{1, 5, 14};{1, 5, 15} {1, 6, 13};{1, 6, 14};{1, 6, 15}
2	$c_6 = 2$, $c_i = 1$ for others	3	{1, 5, 13};{1, 5, 14};{1, 5, 15}
3	$c_6 = 2$, $c_{14} = 1.5$, $c_i = 1$ for others	3	{1, 5, 13};{1, 5, 15}
4	$c_1 = 2$, $c_i = 1$ for others	3	{1, 5, 13};{1, 5, 14};{1, 5, 15} {1, 6, 13};{1, 6, 14};{1, 6, 15}

Based on the results, it is demonstrated that the optimal meter placement solutions may differ if the monitoring cost for each location varies. By comparing case 2 with case 1, it is noticed that the meter placement solutions with bus 6 are no longer optimal solutions since the monitoring cost at bus 6 is higher than that at other locations. In the

third case, the monitoring cost at bus 14 is increased, and as a result, the optimal meter placement solutions containing bus 14 are removed when compared to the solutions of the second case. In case 4, although the monitoring cost at bus 1 is higher than others, the optimal meter placement solutions still contain bus 1. The reason for this is that a meter at bus 1 is mandatory, and $M_1 = 1$. So no matter how high the monitoring cost is, bus 1 is always included in the optimal solutions.

3.6 Summary

This chapter presents fault location observability analysis for distribution systems. Case studies indicate that when limited measurements are available, multiple fault location estimates may exist, which may be impossible to distinguish from the true fault location. Potential techniques by using captured voltage and current measurements are described to trim multiple fault location estimates. To achieve fault location observability of the entire system, sufficient meters are needed to be placed at different locations. An optimal meter placement scheme is proposed to make the distribution system observable while minimizing the total cost or the number of needed meters. The obtained results may provide guidance on installing meters for fault location purposes.

Chapter 4   Optimal Fault Location Estimation in Distribution Systems with DG

A method to optimally estimate fault location on transmission lines is proposed in [59]. This chapter investigates optimal fault location estimation method for distribution systems with DG. In this study, an optimal fault location estimator is presented. It is assumed that measurements at location/locations with power generation are available. This location can either be the substation or location with DG. Approach to detect and identify bad measurement is presented for enhanced accuracy of fault location estimation.

4.1   Fault Location Method

In order to construct the optimal fault location estimator, a fault location method is needed. A previously proposed fault location method described in [10] is employed here for the optimal fault location estimator. The fault location algorithm for LG fault is demonstrated here as an instance. Procedure to find out fault location for other types of fault can be referred to [10]. In this section, it is assumed that measurements at a location with power generation are available. Three nodes at this location are denoted as k_1, k_2 and k_3, respectively.

Based on Figure 2.2, r_1 is added to the faulted phase as the fault node under an LG fault. The voltage change due to the fault at node $k_i, i = 1,2,3$, or superimposed voltage at node k_i, is given as follows [10]:

$$\Delta E_{k_i} = \frac{-E_{p_1 0} + m(E_{p_1 0} - E_{q_1 0})}{A_{11\_0} + A_{11\_1}m + A_{11\_2}m^2 + R_{f_1}}(B_{k_i 1} + C_{k_i 1}m) \qquad (4.1)$$

For the superimposed voltages and currents due to fault at a location with power generation, the following relationship holds [10].

$$[\Delta E] = -[Z_s] \times [\Delta I] \tag{4.2}$$

where

$[\Delta E]$ the three-phase voltage changes due to fault at the location with power generation;

$[\Delta I]$ the three-phase current changes due to fault at the same location;

$[Z_s]$ the source impedance matrix of the source at the same location.

4.2 Optimal Fault Location Estimation

As we know, measurements obtained by recording devices may have errors. Inaccurate measurement data will lead to inaccurate fault location estimates. In order to eliminate the impacts of measurement errors on fault location estimates, an optimal estimator for fault location is proposed in this section. The proposed optimal fault location estimator is capable of detecting and identifying bad measurements.

Optimal fault location estimator for LG faults with available measurements is illustrated here as an example. Optimal fault location estimators for other types of faults can be derived similarly, are not presented here. The study of testing the effectiveness of the optimal fault location estimator is presented in Section 4.4.

Suppose the following vector S is formulated based on the available superimposed voltage and current data caused by the fault:

$$S = [\Delta E_{k_1}, ..., \Delta E_{k_{3N}}, \Delta I_{k_1}, ..., \Delta I_{k_{3N}}]^T \tag{4.3}$$

where

N total number of buses with voltage and current measurements available;

$\Delta E_{k_{3i-2}}, \Delta E_{k_{3i-1}}, \Delta E_{k_{3i}},\quad i=1,2,...,N$ superimposed voltages at bus i, with nodes $k_{3i-2}, k_{3i-1}, k_{3i}$, caused by the fault;

$\Delta I_{k_{3i-2}}, \Delta I_{k_{3i-1}}, \Delta I_{k_{3i}},\quad i=1,2,...,N$ superimposed currents at bus i, with nodes $k_{3i-2}, k_{3i-1}, k_{3i}$, caused by the fault.

Define the unknown variable vector X as

$$X = [x_{1,}x_{2}...,x_{12N},x_{12N+1},x_{12N+2}] \tag{4.4}$$

where

$x_{2i-1}, \quad i=0,...,6N$ magnitude of S_i; S_i is the i_{th} element of S;

$x_{2i}, \quad i=0,...,6N$ angle of S_i;

x_{12N+1} fault location variable;

x_{12N+2} fault resistance variable.

For an LG fault with voltage and current measurements at bus i, $i=0,...,N$, three variable functions (4.5), (4.6), (4.7) can be acquired based on (4.1) and three variable functions (4.8), (4.9), (4.10) can be acquired based on (4.2).

$$f_{3i-2}(X) = \Delta E_{k_{3i-2}}(A_{11\_0} + A_{11\_1}m + A_{11\_2}m^2 + R_{f_1})$$
$$-[-E_{p_1 0} + m(E_{p_1 0} - E_{q_1 0})](B_{k_{3i-2}1} + C_{k_{3i-2}1}m) = 0 \tag{4.5}$$

$$f_{3i-1}(X) = \Delta E_{k_i}(A_{11\_0} + A_{11\_1}m + A_{11\_2}m^2 + R_{f_1})$$
$$-[-E_{p_1 0} + m(E_{p_1 0} - E_{q_1 0})](B_{k_{3i-1}1} + C_{k_{3i-1}1}m) = 0 \tag{4.6}$$

$$f_{3i}(X) = \Delta E_{k_i}(A_{11\_0} + A_{11\_1}m + A_{11\_2}m^2 + R_{f_1})$$
$$-[-E_{p_1 0} + m(E_{p_1 0} - E_{q_1 0})](B_{k_{3i}1} + C_{k_{3i}1}m) = 0 \tag{4.7}$$

$$f_{3N+3i-2}(X) = \Delta E_{k_{3i-2}} + Z_{s\_i}(1,1)\Delta I_{k_{3i-2}} + Z_{s\_i}(1,2)\Delta I_{k_{3i-1}} + Z_{s\_i}(1,3)\Delta I_{k_{3i}} = 0 \tag{4.8}$$

$$f_{3N+3i-1}(X) = \Delta E_{k_{3i-1}} + Z_{s\_i}(2,1)\Delta I_{k_{3i-2}} + Z_{s\_i}(2,2)\Delta I_{k_{3i-1}} + Z_{s\_i}(2,3)\Delta I_{k_{3i}} = 0 \tag{4.9}$$

$$f_{3N+3i}(X) = \Delta E_{k_{3i}} + Z_{s\_i}(3,1)\Delta I_{k_{3i-2}} + Z_{s\_i}(3,2)\Delta I_{k_{3i-1}} + Z_{s\_i}(3,3)\Delta I_{k_{3i}} = 0 \tag{4.10}$$

where Z_{s_i} is the source impedance matrix of the source at bus i. $Z_{s\_i}(a,b)$ represents the element in the a_{th} row and b_{th} column of Z_{s_i}.

From the above derivation, it's known that with measured data at one bus, six variable functions can be formulated. Therefore, a total number of $6N$ variable functions can be constructed based on measurement at N buses.

Define measurement vector Y as

$$Y_i = 0, \quad i = 1,...,12N \tag{4.11}$$

$$Y_{12N+2i-1} = |S_i|, \quad i = 1,...,6N \tag{4.12}$$

$$Y_{12N+2i} = \angle S_i \quad i = 1,...,6N \tag{4.13}$$

where $|.|$ and $\angle.$ represent the magnitude and angle in radiance of the input argument, respectively.

Construct function vector $F(X)$ as

$$F(X) = [\text{Re}(f_1), \text{Im}(f_1), \text{Re}(f_2), \text{Im}(f_2),..., \text{Re}(f_{6N}), \text{Im}(f_{6N}), x_1, x_2,..., x_{12N}]^T$$

(4.14)

where Re(.) and Im(.) represent the real and imaginary part of the input argument, respectively. Both Y and $F(X)$ have a size of 1 by $24N$.

The vector of measurement errors is defined as the difference between measurement vector and function vector as given in (4.15).

$$\mu = Y - F(X)$$
(4.15)

The optimal estimate of X can be achieved with minimized cost function J, which is the determined by the weighting matrix W and measurement errors.

$$J = [Y - F(X)]^T W [Y - F(X)]$$
(4.16)

where the weighing matrix W is the inverse of the covariance matrix R, defined as

$$R = E[\mu\mu^T] = diag[\sigma_1^2, \sigma_2^2,..., \sigma_{4N}^2]$$
(4.17)

In the above equation, $E[.]$ gives the expected value of the input argument. $diag(.)$ is a diagonal matrix with the values in the square brackets. σ_i^2 indicates the error variance of measurement i. The meter with smaller error variance is more accurate.

First, reasonable values for each variable are assigned to X as the initial variable vector X_0. Then, (4.15) is solved iteratively with X being updated by the following procedure [68].

$$H = \left. \frac{\partial F(X)}{\partial X} \right|_{X = X_k} \tag{4.18}$$

$$\Delta X_k = (H^T R^{-1} H)^{-1} \{ H^T R^{-1} [Y - F(X_k)] \} \tag{4.19}$$

$$X_{k+1} = X_k + \Delta X_k \tag{4.20}$$

where

k iteration number starting from 1;

X_k variable vector at k_{th} iteration;

ΔX_k variable update during the k_{th} iteration.

Finally, the optimal solution of X is obtained when the biggest element in the variable update is smaller than the desired tolerance.

4.3 Bad Data Detection

In this dissertation, the Chi-square test is used to determine whether or not bad data exist in the measurement set. The expected value of the cost function is equal to the degrees of freedom K.

$$K = \left| col(H) - row(H) \right| \tag{4.21}$$

where $col(.)$ and $row(.)$ signify the number of columns and rows of the input argument, respectively.

The estimated cost function $\hat{J}$ can be calculated by the following expression:

$$\hat{J} = \sum_{i=1}^{N} \frac{\hat{\mu}_i^{\,2}}{\sigma_i^2} \qquad\qquad (4.22)$$

where

$\hat{\mu}_i$ estimated measurement error in measurement i;

σ_i^2 variance of the error in measurement i;

N total number of measurements.

The Chi-square test, demonstrated in [68], is adopted to determine the presence of a bad data. The Chi-square value with specified probability P of confidence and degrees of freedom K can be found according to the Chi-square distribution table. If $\hat{J} \geq \chi_{K,P}^2$, then bad data will be suspected with probability P. For example, if $\hat{J} \geq \chi_{K,95\%}^2$, it means in 95% of the cases, a bad data exist in the measurements. Then, the measurement with the largest standardized error is identified as the bad data. Otherwise, for cases where $\hat{J} < \chi_{K,P}^2$, the measurement sets are assumed to be free of bad data.

In our study, 0.99 is chosen for P to construct a 99% confidence interval.

4.4 Evaluation Studies

This section presents the evaluation studies on the proposed fault location algorithms. A 18-bus, 12.47kV, 60Hz distribution system, as shown in Figure 4.1, is utilized for the evaluation study. Besides the source at substation, distributed generation are placed at bus 11 and 18, respectively. Single-phase, two-phase, and three-phase laterals and loads are involved. A power factor of 0.9 lagging is assumed for all of the loads. Line length in miles, load ratings in kVA and load phases are clearly labeled. For convenience, base

values of 12.47kV and 1MVA are chosen for the per unit system. In the study, initial

values for variable vector are chosen as: 1.0 p.u. for measurement magnitude, 0 radians

for measurement angle, 0.5 p.u. for fault location and 0.005 p.u. for fault resistances.
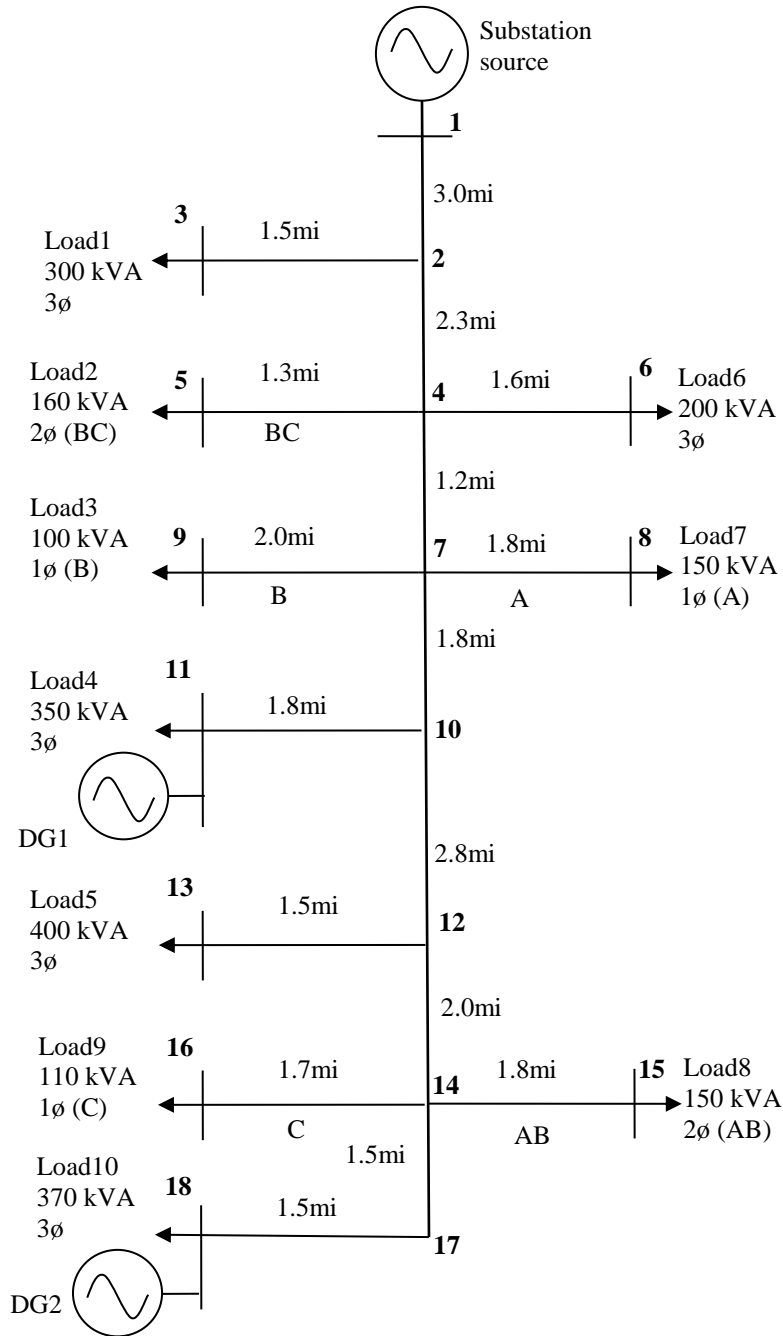
Figure 4.1 A sample power distribution system with DG

Fault location estimates are acquired by implementing the new algorithms in MATLAB [62]. MATLAB tool package SimPowerSystems is utilized to model the studied 18-bus system and generates voltage and current measurements at the substation and locations with DG [62]. Due to different meter accuracies, 10^{-6} and 10^{-4} are chosen as the variance for the first $12N$ measurements and last $12N$ measurements of Y , respectively. In the studies, all the solutions are reached within 10 iterations.

Source impedances for each generator are given as follows. Impedance matrices of main feeders and later feeders in ohms/mile are listed in [63].

Source impedances of substation source:

positive-sequence: 0.23 + j2.10 ohm

zero-sequence: 0.15 + j1.47 ohm

Source impedances of DG1:

positive-sequence: 1.71 + j18.2 ohm

zero-sequence: 1.63 + j17.5 ohm

Source impedances of DG2:

positive-sequence: 2.19 + j22.1 ohm

zero-sequence: 2.05 + j21.6 ohm

The estimation accuracy is evaluated by the percentage error is given in (2.45). The rest of this section presents the fault location results under various studies.

Table 4.1 Fault location results using measurements at substation with faults occurring on

main feeder sections

Fault section	Fault type	Fault location (per unit)	Fault resistance (ohm)	Fault location estimate error (%)	Estimated Fault resistances (ohm)
1-2	LG	0.2	10	0.01	10.00
	LL	0.3	5	0	5.00
	LLG	0.5	[1,1,5]	0.01	[1.00,1.01,5.02]
	LLL	0.7	[5,7,9]	0	[5,7.00,9.00]
	LLLG	0.8	[1,1,1,50]	0	[1.00,1.00,1.00,50.00]
4-7	LG	0.3	5	0.01	5.00
	LL	0.6	1	0	1.00
	LLG	0.7	[2,3,9]	0.05	[1.98,3.03,9.06]
	LLL	0.8	[5,5,5]	0	[9.99,10.00,10.01]
	LLLG	0.3	[5,3,3,20]	0.01	[5.00,3.00,3.00,19.97]
10-12	LG	0.5	1	0.02	1.00
	LL	0.7	10	0	10.00
	LLG	0.1	[1,1,10]	0.03	[1.02,0.98,9.93]
	LLL	0.3	[1,1,1]	0	[1.00,1.00,1.00]
	LLLG	0.4	[2,2,2,10]	0	[2.00,2.00,2.00,9.96]
14-17	LG	0.8	40	0.07	39.91
	LL	0.5	8	0	8.00
	LLG	0.3	[4,2,2]	0.01	[4.00,2.01,2.00]

	LLL	0.4	[2,2,2]	0	[2.00,2.00,2.00]
	LLLG	0.5	[1,2,3,40]	0	[1.00,2.01,3.00,39.15]

Table 4.2 Fault location results using measurements at substation with faults occurring on

lateral feeder sections

Fault section	Fault type	Fault location (per unit)	Fault resistance (ohm)	Fault location estimate error (%)	Estimated Fault resistances (ohm)
2-3	LG	0.7	10	0.02	10.00
	LL	0.2	3	0	3.00
	LLG	0.4	[1,1,5]	0	[1.00,1.00,5.00]
	LLL	0.8	[2,3,4]	0	[2.00,3.00,4.00]
	LLLG	0.6	[4,3,4,25]	0	[4.00,3.00,4.00,24.99]
7-8	LG	0.3	30	0.07	29.99
12-13	LG	0.4	20	0	19.99
	LL	0.6	1	0.01	1.00
	LLG	0.7	[2,3,10]	0.05	[1.96,3.05,10.09]
	LLL	0.2	[3,3,3]	0	[3.00,3.00,3.00]
	LLLG	0.5	[5,5,5,1]	0	[5.00,5.00,5.00,0.92]
14-15	LG	0.3	5	0.02	5.00
	LL	0.5	10	0	10.00
	LLG	0.6	[1,1,5]	0.02	[0.99,1.01,5.02]

Fault location results on different line sections, under different fault types, fault locations and fault resistances are presented in Table 4.1 and Table 4.2. Table 4.1 shows the fault location results using measurements at substation with faults on main feeders. Table 4.2 shows the fault location results using measurements at substation with faults on lateral feeders. The first four columns of Table 4.1 give the actual faulted section, fault type, fault location in per unit and fault resistance in ohms, respectively. Estimates of fault location errors and estimated fault resistances are given in the last two columns. Both balanced and unbalanced LLL and LLLG faults are considered in the study. In this section, fault location estimation error equals 0 indicates the error is less than 0.005 in percentage.

From the above tables, it is evinced that accurate results have been achieved by the proposed optimal fault location estimator. Biggest fault location error is 0.07%.

Fault location results using voltage and current data at substation and locations with DG are displayed in Table 4.3 and 4.4. Fault location estimation under the same faults as those shown in Table 4.1 and 4.2 are displayed in Table 4.3 and 4.4, respectively. From Table 4.3 and 4.4 it is learned that, accuracy of fault location estimates can be enhanced if more measurements are available. All fault location errors are within 0.07%.

Table 4.3 Fault location results using measurements at substation and locations with DG

with faults occurring on main feeder sections

Fault section	Fault type	Fault location (per unit)	Fault resistance (ohm)	Fault location estimate error (%)	Estimated Fault resistances (ohm)
1-2	LG	0.2	10	0.01	10.00
	LL	0.3	5	0	5.00
	LLG	0.5	[1,1,5]	0	[1.00,1.01,5.02]
	LLL	0.7	[5,7,9]	0	[5.00,7.00,9.00]
	LLLG	0.8	[1,1,1,50]	0	[1.00,1.00,1.00,50.00]
4-7	LG	0.3	5	0.01	5.00
	LL	0.6	1	0	1.00
	LLG	0.7	[2,3,9]	0	[1.99,3.01,8.98]
	LLL	0.8	[5,5,5]	0	[10.00,10.00,10.00]
	LLLG	0.3	[5,3,3,20]	0	[5.00,3.00,3.00,19.99]
10-12	LG	0.5	1	0	1.00
	LL	0.7	10	0	10.00
	LLG	0.1	[1,1,10]	0.02	[1.00,1.00,10.00]
	LLL	0.3	[1,1,1]	0	[1.00,1.00,1.00]
	LLLG	0.4	[2,2,2,10]	0	[2.00,2.00,2.00,10.00]
14-17	LG	0.8	40	0.05	40.01
	LL	0.5	8	0	8.00
	LLG	0.3	[4,2,2]	0.01	[4.00,2.00,2.00]

| | LLL | 0.4 | [2,2,2] | 0 | [2.00,2.00,2.00] |
| | LLLG | 0.5 | [1,2,3,40] | 0 | [1.00,2.00,3.00,40.22] |

Table 4.4 Fault location results using measurements at substation and locations with DG

with faults occurring on lateral feeder sections

Fault section	Fault type	Fault location (per unit)	Fault resistance (ohm)	Fault location estimate error (%)	Estimated Fault resistances (ohm)
2-3	LG	0.7	10	0.01	10.00
	LL	0.2	3	0	3.00
	LLG	0.4	[1,1,5]	0	[1.00,1.00,5.00]
	LLL	0.8	[2,3,4]	0	[2.00,3.00,4.00]
	LLLG	0.6	[4,3,4,25]	0	[4.00,3.00,4.00,25.00]
7-8	LG	0.3	30	0.07	30.01
12-13	LG	0.4	20	0	20.00
	LL	0.6	1	0	1.00
	LLG	0.7	[2,3,10]	0.02	[1.99,3.01,9.99]
	LLL	0.2	[3,3,3]	0	[3.00,3.00,3.00]
	LLLG	0.5	[5,5,5,1]	0	[5.00,5.00,5.00,0.988]
14-15	LG	0.3	5	0	5.00
	LL	0.5	10	0	10.00
	LLG	0.6	[1,1,5]	0	[1.00,1.00,5.00]

The effectiveness of the proposed optimal estimator in detecting and identifying existing bad measurement has been studied and results are demonstrated as follows. Suppose that an AG fault with 0.3 p.u. fault location and 5 Ohm fault resistance takes place on line section 4-7 of the simulated power system. Measurements at the local substation are employed for the optimal fault location estimator.

After voltage and current measurements are extracted from MATLAB model, the voltage magnitude of phase A at substation is deliberately multiplied by 1.5 to generate a bad measurement. Optimal estimations of all variables in the variable vector with bad measurement are presented in Table 4.5. Optimal estimations of variables after the bad data is removed are displayed in Table 4.6. The first three columns of Table 4.5 and 4.6 list the available measurements, measurement units, measured values, respectively. Optimal estimates of all variables are given in the last column.

According to (2.45), fault location error is obtained as 14.47%, which is considerably large. After calculating the cost function and looking up in the table for Chi-square distribution, it can be acquired that $\hat{J} = 1007.9491$ and $\chi^2_{10,0.99} = 23.2093$. Since $\hat{J} \geq \chi^2_{k,p}$, a bad measurement is detected. Searching for the measurement with the biggest standard error, bad measurement is identified as the measured voltage magnitude of phase A at the local substation. After eliminating the bad data, and use the rest data to perform optimal estimation again, the results in Table 4.6 are obtained. "N/A" indicates the corresponding value is not available.

Table 4.5 Optimal estimates using measurements at substation with bad voltage

measurement at $\left|\Delta E_1\right|$

Quantity	Unit	Measured values	Optimal estimates
$\left\|\Delta E_1\right\|$	per unit	0.2157	0.2925
$\angle\Delta E_1$	radians	-2.3658	-2.3659
$\left\|\Delta E_2\right\|$	per unit	0.0373	0.0399
$\angle\Delta E_2$	radians	0.7856	0.7855
$\left\|\Delta E_3\right\|$	per unit	0.0330	0.0370
$\angle\Delta E_3$	radians	0.7433	0.7435
$\left\|\Delta I_1\right\|$	per unit	0.1741	0.2113
$\angle\Delta I_1$	radians	-0.6876	-0.6876
$\left\|\Delta I_2\right\|$	per unit	0.0122	0.0129
$\angle\Delta I_2$	radians	2.5047	2.5047
$\left\|\Delta I_3\right\|$	per unit	0.0089	0.0103
$\angle\Delta I_3$	radians	2.4009	2.4009
m	per unit	0.3000	-1.4359
R_f	per unit	3.2154	2.7166

Table 4.6 Optimal estimates using measurements at substation with bad voltage

measurement removed

Quantity	Unit	Measured values	Optimal estimates
$\left\lvert\Delta E_1\right\rvert$	per unit	N/A	0.2157
$\angle\Delta E_1$	radians	-2.3658	-2.3659
$\left\lvert\Delta E_2\right\rvert$	per unit	0.0373	0.0374
$\angle\Delta E_2$	radians	0.7856	0.7857
$\left\lvert\Delta E_3\right\rvert$	per unit	0.0330	0.0330
$\angle\Delta E_3$	radians	0.7433	0.7433
$\left\lvert\Delta I_1\right\rvert$	per unit	0.1741	0.1741
$\angle\Delta I_1$	radians	-0.6876	-0.6876
$\left\lvert\Delta I_2\right\rvert$	per unit	0.0122	0.0122
$\angle\Delta I_2$	radians	2.5047	2.5047
$\left\lvert\Delta I_3\right\rvert$	per unit	0.0089	0.0090
$\angle\Delta I_3$	radians	2.4009	2.4009
m	per unit	0.3000	0.3023
R_f	per unit	3.2154	3.2142

After removing the bad data, the newly calculated cost function $\hat{J} = 0.0193$ and $\chi^2_{8,0.99} = 20.0902$. Fault location error after bad data being removed is 0.02%. As a result, the new measurement sets are considered free of bad data, and the fault location estimate is shown to be very accurate. Optimal estimates of variables based on measurements at substation and locations with DG are also very accurate.

Optimal estimates with error in current measurements have also been tested. Suppose the same fault, AG fault with 0.3 p.u. fault location and 5 Ohm fault resistance, occurs in the system. Bad measurement is generated by multiplying the current magnitude of phase A by 1.5. All other measurements are accurate. Optimal estimations of all variables in the variable vector with bad measurement are presented in Table 4.7.

By comparing the values of estimated cost function and Chi-square value, measured current magnitude of phase A at the local substation is detected with measurement error. Optimal estimation results after removing the bad data are listed in Table 4.8.

Table 4.7 Optimal estimates using measurements at substation with bad current

measurement at $\left| \Delta I_1 \right|$

Quantity	Unit	Measured values	Optimal estimates
$\left\| \Delta E_1 \right\|$	per unit	0.2157	0.2457
$\angle \Delta E_1$	radians	-2.3658	-2.3659
$\left\| \Delta E_2 \right\|$	per unit	0.0373	0.0380
$\angle \Delta E_2$	radians	0.7856	0.7856
$\left\| \Delta E_3 \right\|$	per unit	0.0330	0.0343
$\angle \Delta E_3$	radians	0.7433	0.7434
$\left\| \Delta I_1 \right\|$	per unit	0.1741	0.2243
$\angle \Delta I_1$	radians	-0.6876	-0.6876
$\left\| \Delta I_2 \right\|$	per unit	0.0122	0.0072
$\angle \Delta I_2$	radians	2.5047	2.5047
$\left\| \Delta I_3 \right\|$	per unit	0.0089	0.0043
$\angle \Delta I_3$	radians	2.4009	2.4009
m	per unit	0.3000	-0.5305
R_f	per unit	3.2154	3.0142

Table 4.8 Optimal estimates using measurements at substation with bad current

measurement removed

Quantity	Unit	Measured values	Optimal estimates
$\left\vert\Delta E_1\right\vert$	per unit	0.2157	0.2157
$\angle\Delta E_1$	radians	-2.3658	-2.3658
$\left\vert\Delta E_2\right\vert$	per unit	0.0373	0.0374
$\angle\Delta E_2$	radians	0.7856	0.7857
$\left\vert\Delta E_3\right\vert$	per unit	0.0330	0.0330
$\angle\Delta E_3$	radians	0.7433	0.7433
$\left\vert\Delta I_1\right\vert$	per unit	N/A	0.1741
$\angle\Delta I_1$	radians	-0.6876	-0.6877
$\left\vert\Delta I_2\right\vert$	per unit	0.0122	0.0122
$\angle\Delta I_2$	radians	2.5047	2.5047
$\left\vert\Delta I_3\right\vert$	per unit	0.0089	0.0089
$\angle\Delta I_3$	radians	2.4009	2.4009
m	per unit	0.3000	0.3008
R_f	per unit	3.2154	3.2146

After current magnitude of phase A being eliminated from the measurement pool, no other bad data are found based on the newly calculated cost function and Chi-square value. As can be seen from Table 4.8, fault location estimate is very accurate.

Optimal fault location estimation based on measurements at substation and locations with DG yield similar accurate results.

4.5 Summary

This chapter describes a novel optimal fault location estimator for distribution systems with DG. Voltage and current measurements at substation with/without measurements at locations with DG are utilized to give the best estimation of all available measurements along with fault location and fault resistances. Functions of superimposed measurements, fault location and fault resistance are obtained based on the characteristics of the system. Then, estimation of all variables is evaluated iteratively. Simulation studies have demonstrated that highly accurate estimates are obtained. If a bad measurement exists in the measured data, the proposed method is able to detect and identify this bad measurement successfully. Fault location estimates after removing the bad data from the data pool are very accurate.

Chapter 5   Conclusions

Faults on power systems may result in discontinue of electricity, which will do harm to schools, hospitals, and public safety entities including, police stations, fire department, law enforcement agencies, etc. Failure of power also brings the country financial losses.

Impedance based fault location methods for radial and non-radial ungrounded distribution systems are proposed in Chapter 2. Fault location methods using line to neutral voltages at substation are presented first. When line to line to neutral voltages are not available due to physical connection inside the sources, fault location approaches using line to line voltages at substation are utilized as an alternative. Voltages at substation nodes are formulated as the functions of bus impedance matrix and current at the substation. Bus impedance matrix contains the fault location to be determined. By solving the constructed function with measured voltages at the substation, fault location can be estimated. For both radial and non-radial ungrounded distribution systems, fault location methods for LL and LLL faults are designed, where the former ones do not have to be solved iteratively. In fault location methods for non-radial ungrounded distribution systems, pre-fault node voltages and source impedance is not required. Evaluations studies on 12.47 kV 16-bus radial system and 17-bus non-radial system are carried out. Accurate fault location estimates are obtained by both methods. The proposed fault location methods are very robust to load variation and measurement data with errors.

Due to presence of multi-laterals in distribution systems, and limited monitoring devices, it may be inherently impossible to uniquely determine some fault locations. In other words, there may be multiple fault location estimates if only a limited measurements are available, and all such estimates satisfy the given network conditions

and measurements. Optimal meter placement method to minimize the number of meters needed while make every fault location uniquely determinable by available measurement. In this dissertation, an optimal meter deployment problem is converted into an integer linear programming, as shown in Chapter 3. At first, the constraints corresponding to a certain fault location under a specified type of fault and fault resistance is formulated. Then, the constraints for all the other fault locations and resistances under the same fault type can be acquired similarly. In the end, the constraints for all fault locations under all types of faults and fault resistances are obtained. By minimizing the objective function subject to all of the constraints, the optimal meter placement problem can be solved. All constrains are formulated based on the results of fault location observability analysis. An existing fault location algorithm is adopted for fault location observability study, and measurements at only one bus are required to find the fault location. Fault location methods for LG, LL, LLG, LLL and LLLG are presented. Evaluation studies are performed on a 12.47kV 16-bus distribution system. For a fault location in the system, measured voltages at one bus may results in two or more possible fault locations. In this case, more meters are needed to make the actual fault location observable. Evaluation studies demonstrate that the length and number of unobservable segments in the system can be largely reduced by installing more meters in the system. To make the entire studied distribution system observable, four meters are needed at specific locations. In other words, four meters at specified locations are enough to locate any fault in the system.

A method to optimally estimate the unknown fault location in distribution systems is described in Chapter 4. The proposed methods employ voltage and current

measurements at substation with/without locations with DG to determine the best estimation of measurements, fault location and fault resistances. Optimal estimation of all variables, including fault location, fault resistances and measurements, are acquired by iteratively solve the functions obtained based on the characteristic of the system. Very accurate fault location estimates are obtained according to the evaluation studies. This dissertation also provides a method to detect and identify bad measurement if there is any in the measured data. Evaluation study indicates that bad measurement can be detected by comparing the value of cost function with the Chi-square value. Then, bad date is identified as the one with largest standardized error. After removing the bad measurement from the measurement poor, and use the rest of the measurements to estimate fault location again, very accurate fault location estimates are obtained.

References

[1] D. Jalali and N. Moslemi, "Fault location for radial distribution system using fault generated high-frequency transients and wavelet analysis," 18th International Conference and Exhibition on Electricity Distribution, Turin, Italy, June 6-9, 2005.

[2] J. Sadeh, E. Bakhshizadeh, and R. Kazemzadeh, "New fault location algorithm for radial distribution systems using modal analysis," International Journal of Electrical Power and Energy Systems, vol. 45, pp. 271-278, February 2013.

[3] A. M. El-Zonkoly, "Fault diagnosis in distribution networks with distributed generation," Electric Power Systems Research, vol. 81, no. 7, pp. 1482-1490, July 2011.

[4] L. Zewen, H. Huanhuan and D. Feng, "Power grid fault traveling wave network location method," 2013 IEEE Industry Applications Society Annual Meeting, Lake Buena Vista, FL, October 06-11, 2013.

[5] H. Nouri, C. Wang, and T. Davies, "An accurate fault location technique for distribution lines with tapped loads using wavelet transform," IEEE Porto Power Tech Conference, Porto, Portugal, September 10-13, 2001.

[6] H. Li, A. S. Mokhar, and N. Jenkins, "Automatic fault location on distribution network using voltage sags measurements," 18th International Conference and Exhibition on Electricity Distribution, Turin, Italy, June 6-9, 2005.

[7] R. A. F. Pereira, L. G. W. Silva, M. Kezunovic, and J. R. S. Mantovani, "Improved fault location on distribution feeders on matching during-fault voltage sags," IEEE Transactions on Power Delivery, vol. 24, no. 2, pp. 852-862, April 2009.

[8] S. Lotfifard, M. Kezunovic, and M.J. Mousavi, "Voltage sag data utilization for distribution fault location," IEEE Transactions on Power Delivery, vol. 26, no. 2, pp 1239-1246, April 2011.

[9] N. Kang; Y. Liao, "Fault location estimation for transmission lines using voltage sag data," 2010 IEEE Power and Energy Society General Meeting, Minneapolis, MN, July 25-29, 2010.

[10] Y. Liao, "Generalized fault-location methods for overhead electric distribution systems," IEEE Transactions on Power Delivery, vol. 26, no. 1, pp. 53-64, January 2011.

[11] R. Das, M. S. Sachdev, and T. S. Sidhu, "A fault locator for radial sub-transmission and distribution lines," 2000 IEEE Power Engineering Society Summer Meeting, Seattle, Washington, July 16-20, 2000.

[12] R. K. Aggarwal, Y. Aslan, and A. T. Johns, "New concept in fault location for overhead distribution systems using superimposed components," IEE Proceedings on Generation, Transmission and Distribution, vol. 144, no. 3, pp. 309-316, May 1997.

[13] R. K. Aggarwal, Y. Aslan, and A. T. Johns, "An interactive approach to fault location on overhead distribution lines with load taps," 6th International Conference on Developments in Power System Protection, pp. 184-187, Nottingham , March 25-27, 1997.

[14] A. L. Dalcastagne, S. N. Filho, H. H. Zurn, and R. Seara, "An iterative two-terminal fault-location method based on unsynchronized phasors," IEEE Transaction on Power Delivery, vol. 23, no. 4, pp. 2318–2329, October 2008.

[15] J. Kim, M. Baran, and G. Lampley, "Estimation of fault location on distribution feeders using PQ monitoring data," IEEE Power Engineering Society General Meeting, Tampa, FL, June 24-28, 2007.

[16] J. Teng, W. Huang and S. Luan, "Automatic and fast faulted line-section location method for distribution systems based on fault indicators," IEEE Transactions on Power Systems, vol. 29, no. 4, pp. 1653-1662, July 2014.

[17] S. Lotfifard, M. Kezunovic, and M. J. Mousavi, "A systematic approach for ranking distribution systems fault location algorithms and eliminating false estimates," IEEE Transactions on Power Delivery, vol. 28, no. 1, pp. 285-293, January 2013.

[18] J. Zhu, D. L. Lubkeman, and A. A. Girgis, "Automated fault location and diagnosis on electric power distribution feeders," IEEE Transactions on Power Delivery, vol. 2, no. 2, pp. 801-809, April 1997.

[19] R. Krishnathevar and E. E. Ngu, "Generalized impedance-based fault location for distribution systems," IEEE Transactions on Power Delivery, vol. 27, no. 1, pp. 449-451 January 2012.

[20] G. Morales-España, J. Mora-Flórez, and H. Vargas-Torres, "Elimination of multiple estimation for fault location in radial power systems by using fundamental single-end measurements," IEEE Transactions on Power Delivery, vol. 24, no. 3, pp. 1382-1389, July 2009.

[21] F. Yan, W. Liu, and L. Tian, "Fault location for 10kV distribution line based on traveling wave-ANN theory," 2011 IEEE Power Engineering and Automation Conference, vol. 2, pp. 437-440, September 8-9, 2011.

[22] L. S. Martins, J. F. Martins, C. M. Alegria, and V. Femilo Pires, "A network distribution power system fault location based on neural eigenvalue algorithm," 2003 IEEE Bologna Power Tech Conference, Bologna, Italy, June 23–26, 2003.

[23] F. Dehghani and H. Nezami, "A new fault location technique on radial distribution systems using artificial neural network," 22nd International Conference and Exhibition on Electricity Distribution, pp. 1-4, Stockholm, June 10-13, 2013.

[24] J. J. Mora, G. Carrillo, and L. Perez, "Fault location in power distribution systems using ANFIS nets and current patterns," 2006 IEEE/PES Transmission and Distribution Conference and Exposition: Latin America, pp. 1–6, Caracas, August 15-18, 2006.

[25] X. Zhu, X. Lu, D. Liu, and B. Zhang, "An improved fault locating system of distribution network based on fuzzy identification," 2010 China International Conference on Electricity Distribution, pp. 1-6, Nanjing, China, September 13-16, 2010.

[26] J. Mora-Florez, V. Barrera-Nuez, and G. Carrillo-Caicedo, "Fault location in power distribution systems using a learning algorithm for multivariable data analysis," IEEE Transactions on Power Delivery, vol. 22, no. 3, pp.1715-1721, July, 2007.

[27] M. M. Hosseini, M. T. Hagh, and S. Asgarifar, "A novel fault location algorithm for double fed distribution networks," IEEE Power Engineering and Automation Conference (PEAM), 2011.

[28]   M. S. Choi, S. J. Lee, D. S. Lee, and B. G. Jin, "A new fault location algorithm using direct circuit analysis for distribution systems," IEEE Transactions on Power Delivery, vol. 19, no. 1, pp. 35-41, January 2004.

[29]   M. S. Choi, S. J. Lee, S. I. Lim, D. S. Lee, and X. Yang, "A direct three-phase circuit analysis-based fault location for line-to-line fault," IEEE Transactions on Power Delivery, vol. 22, no. 4, pp. 2541-547, October 2007.

[30]   A. A. Girgis, C. M. Fallon, and D. L. Lubkeman, "A fault location technique for rural distribution feeders," IEEE Transactions on Industry Applications, vol. 29, no. 6, pp. 1170-1175, November/December 1993.

[31]   G. D. Ferreira, D. S. Gazzana, A. S. Bretas, and A. S. Netto, "A unified impedance-based fault location method for generalized distribution systems," Power and Energy Society General Meeting, San Diego, CA, July 2012.

[32]   D. Novosel, D. Hart, and J. Myllymaki, "System for locating faults and estimating fault resistance in distribution networks with tapped loads," U.S. Patent 5839093, 1998.

[33]   T. A. Kawady, A.-M. I. Taalab and M. El-Sad, "An accurate fault locator for underground distribution networks using modified apparent-impedance calculation," 10th IET International Conference on Developments in Power System Protection, pp. 1-5, Manchester, March 29-April 1, 2010.

[34]   S. Kulkarni, S. Santoso, and, T. A. Short, "Incipient Fault Location Algorithm for Underground Cables," IEEE Transactions on Smart Grid, vol. 5, no. 3, pp. 1165-1174, May 2014.

[35]   T. S. Sidhu; Z. Xu, "Detection of Incipient Faults in Distribution Underground Cables," IEEE Transactions on Power Delivery, vol. 25, no. 3, pp. 1363-1371, July 2010.

[36]   Z. Xu, "Fault location and incipient fault detection in distribution cables," Ph.D. dissertation, Electrical and Computer Engineering, University of Western Ontario, London, Ontario, 2011.

[37]   J. Moshtagh and R.K. Aggarwal, "A new approach to ungrounded fault location in a three-phase underground distribution system using combined neural networks and wavelet analysis," 2006 Canadian Conference on Electrical and Computer Engineering, pp. 376-381, Ottawa, ON, Canada, May 2006.

[38]   S. Nam, S. Kang, J. Sohn, and J. Park, "Ground-fault location algorithm for ungrounded radial distribution systems", Electrical Engineering, vol. 89, no. 6, pp. 503-508, June 2007.

[39]   H. Sun, D. Nikovski, T. Takano, Y. Kojima, and T. Ohno, "Fault location analysis of ungrounded distribution system based on residual voltage distribution," 2013 North American Power Symposium, pp. 1-6, Manhattan, KS, September 22-24, 2013.

[40]   T. Baldwin, F. Renovic, L. Saunders, and D. Lubkeman, "Fault locating in ungrounded and high-resistance grounded systems," 2001 IEEE Industrial and Commercial Power Systems Technical Conference, pp. 163-169, New Orleans, LA, May 2001.

[41]   A. A. P. Bíscaro, R. A. F. Pereira, and J. R. S. Mantovani, "Optimal phasor measurement units placement for fault location on overhead electric power

distribution feeders," 2010 IEEE/PES Transmission and Distribution Conference and Exposition: Latin America (T&D-LA), pp. 37-43, Sao Paulo, November 8-10, 2010.

[42]   R. A. F. Pereira, L. G. W. Da Silva, and J. R. S. Mantovani, "PMUs optimized allocation using a tabu search algorithm for fault location in electric power distribution system," 2004 IEEE/PES Transmission and Distribution Conference and Exposition: Latin America, pp.143-148, November 8-11, 2004.

[43]   M. Oleskovicz, H. M. G. C. Branco, R. P. M. da Silva, D. V. Coury, and A. C. B. Delbem, "A compact genetic algorithm structure used for the optimum allocation of power quality monitors based on electrical circuit topology," 2012 IEEE 15th International Conference on Harmonics and Quality of Power (ICHQP), Hong Kong, China, June 17-20, 2012.

[44]   C. Ho, T. Lee, and C. Lin, "Optimal Placement of Fault Indicators Using the Immune Algorithm," IEEE Transactions on Power Systems, vol. 26, no. 1, pp. 38-45, February 2011.

[45]   K. Lien, C. Liu, and C. Yu, J. Jiang, "Transmission network fault location observability with minimal PMU placement," IEEE Transactions on Power Delivery, vol. 21, no. 3, pp. 1128-1136, July 2006.

[46]   M. Korkali and A. Abur, "Optimal deployment of wide-area synchronized measurements for fault-location observability," IEEE Transactions on Power Systems, vol. 28, no. 1, pp. 482-489, February 2013.

[47]   K. Mazlumi, H. Askarian Abyaneh, S. H. H. Sadeghi, and S. S. Geramian, "Determination of optimal PMU placement for fault-location observability," 2008

Third International Conference on Electric Utility Deregulation and Restructuring and Power Technologies, pp. 1938-1942, Nanjing, China, April 6-9, 2008.

[48]   Y. Liao, "Fault location observability analysis and optimal meter placement based on voltage measurements," Electric Power Systems Research, vol. 79, no. 7, pp. 1026-1068, July 2009.

[49]   M. Avendaño-Mora and J. V. Milanović, "Generalized formulation of the optimal monitor placement problem for fault location," Electric Power Systems Research, vol. 93, pp. 120-126, December 2012.

[50]   F. de Santana, L. A L De Almeida, and F. F. Costa, "Optimal positioning of geo-referenced short circuit sensors for faster fault finding using genetic algorithm," 2008 IEEE International Symposium on Industrial Electronics, Cambridge, England, June 30-July 2, 2008.

[51]   M. C. de Almeida, F. F. Costa, S. Xavier-de-Souza and F. Santana, "Optimal placement of faulted circuit indicators in power distribution systems," Electric Power Systems Research, vol. 81, no. 2, pp. 699-706, February 2011.

[52]   J. Suonan and J. Qi, "An accurate fault location algorithm for transmission line based on R–L model parameter identification," Electric Power Systems Research, vol. 76, no. 1-3, pp. 17-24, September 2005.

[53]   M. da Silva, M. Oleskovicz, and D.V. Coury, "A hybrid fault locator for three-terminal lines based on wavelet transforms," Electric Power Systems Research, vol. 78, no. 11, pp. 1980-1988, November 2008.

[54] S. Kang, Y. Ahn, Y. Kang, and S. Nam, "A fault location algorithm based on circuit analysis for untransposed parallel transmission lines," IEEE Transactions on Power Delivery, vol. 24, no. 4, pp. 1850-1856, October 2009.

[55] S. F. Mekhamer, A. Y. Abdelaziz, M. Ezzat, and T. S. Abdel-Salam, "Fault location in long transmission lines using synchronized phasor measurements from both ends," Electric Power Components and Systems, vol. 40, no. 7, pp. 759-776, April 2012.

[56] Wanjing Xiu, Yuan Liao, "Novel fault location methods for ungrounded radial distribution systems using measurements at substation," Electric Power System Research, vol. 106, pp. 95-100, January 2014.

[57] Wanjing Xiu, Yuan Liao, "Fault location methods for ungrounded distribution systems using local measurements," International Journal of Emerging Electric Power Systems, vol. 14, no. 5, pp. 467–476, August 2013.

[58] J. Grainger and W. Stevenson, Power System Analysis. New York: McGraw-Hill, 1994.

[59] Y. Liao and M. Kezunovic, "Optimal Estimate of Transmission Line Fault Location Considering Measurement Errors," IEEE Transactions on Power Delivery, vol. 22, no. 3, pp. 1335-1341, July 2007.

[60] E. Makram, M. Bou-Rabee, and A. Girgis, "Three-phase modeling of unbalanced distribution system during open conductors and/or shut fault conditions using the bus impedance matrix," Electric Power System Research, vol.13, no. 3, pp. 173-183, December 1987.

[61] C. S. Cheng and D. Shirmohammadi, "A three-phase power flow method for real-time distribution system analysis," IEEE Transactions on Power Systems, vol. 10, no. 2, pp. 671-679, May 1995.

[62] MATLAB User Guides, The MathWorks, Inc., 2009.

[63] W. H. Kersting, "Radial distribution test feeders," IEEE Power Engineering Society Winter Meeting, Columbus, OH, January 28-February 1, 2001.

[64] G. N. Korres, N. M. Manousakis, "A state estimation algorithm for monitoring topology changes in distribution systems," IEEE Power and Energy Society General Meeting, San Diego, CA, July 22-26, 2012.

[65] G. Olguin, F. Vuinovich, and M. Bollen, "An optimal monitoring program for obtaining voltage sag system indexes," IEEE Transactions on Power Systems, vol. 21, no. 1, pp. 378-384, February 2006.

[66] H. P. Williams, Model Building in Mathematical Programming, John Wiley & Sons Ltd., West Sussex, England, 1999.

[67] ILOG, Inc., ILOG CPLEX 9.1 User's Manual, 2005.

[68] A. Abur and A. G. Exposito, Power system state Estimation: Theory and Implementation. New York: Marcel Dekker, 2004.

VITA

Wanjing Xiu

Date and place of birth

Wanjing Xiu was born in Wuhan, Hubei Province, P. R. China.

Education

08/2009—present

Ph. D. Student

Department of Electrical and Computer Engineering, University of Kentucky, Lexington, Kentucky, USA

08/2009—Fall 2012

Master of Engineering

Department of Electrical and Computer Engineering, University of Kentucky, Lexington, Kentucky, USA

09/2005—07/2009

Bachelor of Engineering

Department of Electrical and Telecommunication Engineering, Huazhong University of Science and Technology (HUST), Wuhan, Hubei, P. R. China

Awards

08/2010—present

Researching Assistant, Power and Energy Institute of Kentucky (PEIK), University of

Kentucky, Lexington, KY, USA

08/2009—07/2010

Teaching Assistant, University of Kentucky, Lexington, KY, USA

09/2005—07/2009

Student Scholarship, HUST, Wuhan, Hubei, P. R. China

Publications

1. Wanjing Xiu, Yuan Liao, "Novel fault location methods for ungrounded radial distribution systems using measurements at substation," Electric Power System Research, vol. 106, pp. 95-100, January 2014.

2. Wanjing Xiu, Yuan Liao, "Fault location methods for ungrounded distribution systems using local measurements," International Journal of Emerging Electric Power Systems, vol. 14, no. 5, pp. 467–476, August 2013.

3. Wanjing Xiu, Yuan Liao, "Fault location for parallel transmission lines with limited voltage and current measurements," International Journal of Emerging Electric Power Systems, vol. 14, no. 3, pp. 265–274, June 2013.

4. Wanjing Xiu, Yuan Liao, "Power system planning studies on a real utility system," Journal of Computers, vol. 8, no. 1, pp 79-84, January 2013.

5. Wanjing Xiu, Yuan Liao, "Online one-end fault location algorithm for parallel transmission lines," Smart Grid and Renewable Energy, vol. 2, no. 4, pp. 359-366, November 2011.

6. Wanjing Xiu, Yuan Liao, "Accurate transmission line fault location considering shunt capacitances without utilizing line parameters," Electric Power Components and Systems, vol. 39, no. 16, pp. 1783-1794, October 2011.

7. Wanjing Xiu,Yuting Zhang, "Substation design for railway safety wireless forewarning system," Computer and Communications , vol. 26, no. 6, December 2008.